Exosomal Tumor MicroRNA Modulates Premetastatic Organ Cells[1,2]

Sanyukta Rana[*], Kamilla Malinowska[*] and Margot Zöller[*,†]

[*]Department of Tumor Cell Biology, University Hospital of Surgery, Heidelberg, Germany; [†]German Cancer Research Center, Heidelberg, Germany

Abstract

Tumor exosomes educate selected host tissues toward a prometastatic phenotype. We demonstrated this for exosomes of the metastatic rat adenocarcinoma BSp73ASML (ASML), which modulate draining lymph nodes and lung tissue to support settlement of poorly metastatic BSp73ASML-CD44v4-v7 knockdown (ASML-CD44v[kd]) cells. Now, we profiled mRNA and microRNA (miRNA) of ASML[wt] and ASML-CD44v[kd] exosomes to define the pathway(s), whereby exosomes prepare the premetastatic niche. ASML exosomes, recovered in draining lymph nodes after subcutaneous injection, preferentially are taken up by lymph node stroma cells (LnStr) and lung fibroblasts (LuFb) that were chosen as exosome targets. ASML[wt] and ASML-CD44v[kd] exosomes contain a restricted mRNA and miRNA repertoire that differs significantly between the two lines and exosomes thereof due to CD44v6 influencing gene and miRNA transcription/posttranscriptional regulation. Exosomal mRNA and miRNA are recovered in target cells, where transferred miRNA significantly affected mRNA translation. Besides others, this was exemplified for abundant ASML[wt]-exosomal miR-494 and miR-542-3p, which target cadherin-17 (cdh17). Concomitantly, matrix metalloproteinase transcription, accompanying cdh17 down-regulation, was upregulated in LnStr transfected with miR-494 or miR-542-3p or co-cultured with tumor exosomes. Thus, tumor exosomes target non-transformed cells in premetastatic organs and modulate premetastatic organ cells predominantly through transferred miRNA, where miRNA from a metastasizing tumor prepares premetastatic organ stroma cells for tumor cell hosting. Fitting the demands of metastasizing tumor cells, transferred exosomal miRNA mostly affected proteases, adhesion molecules, chemokine ligands, cell cycle– and angiogenesis-promoting genes, and genes engaged in oxidative stress response. The demonstration of function-competent exosomal miRNA in host target cells encourages exploiting exosomes as a therapeutic gene delivery system.

Neoplasia (2013) 15, 281–295

Introduction

Metastasis formation accounts for the majority of cancer-induced deaths, where a given tumor type preferentially seeds in selected organs [1,2]. Premetastatic niche preparation supports the seed and soil hypothesis, as tumors prepare only defined organs for metastasizing cell settlement in advance of arrival [3–5]. Our suggestion that tumor-derived exosomes rather than individual molecules play an important role [6] was confirmed by several groups [7–16]. Exosomal microRNA (miRNA) in serum is also discussed as a potential marker for tumor diagnosis [17,18].

Exosomes, small vesicles delivered by many cells and abundantly by tumor cells [19], derive from early endosomes, which fuse to multivesicular bodies (MVBs), from where individual vesicles (exosomes) are released in the extracellular space [20–23]. Accordingly, exosomes are

rich in proteins located in internalization-prone membrane domains and molecules engaged in fission, scission, and vesicular transport [14,22,24,25]. Exosomes also harbor selected mRNA and miRNA [26]. mRNA recruitment may be guided by a zip code in the 3′ untranslated region (3′UTR) [27]; miRNA recruitment is facilitated by physical and functional coupling of RNA-induced silencing complexes to components of the sorting complex, where GW182 containing GW bodies, sorted into MVB, promotes continuous assembly/disassembly of membrane-associated miRNA-loaded RNA-induced silencing complex [28,29].

Exosome binding and uptake by target cells are also selective processes that involve various endocytic pathways and proteins from exosome donor and target cells [30,31], where exosomal tetraspanin complexes bind to selected ligands, which are also located in internalization-prone microdomains [32,33]. Exosomal proteins, mRNA, and miRNA are functionally active [22,34,35] and exosome binding/uptake can severely alter target cells, as demonstrated for T cell activation, immunosuppression, and conversion to a malignant phenotype [14,36–38].

We showed for the metastasizing rat pancreatic adenocarcinoma BSp73ASML (ASML) [39] that exosomes contribute to premetastatic niche preparation. ASML cells highly express CD44 variant isoforms v4–v7 (CD44v) [6], where CD44v6 particularly promotes the metastatic phenotype [40]. First evidence for CD44v as a metastasis-promoting molecule deriving from metastasis formation of CD44v transfected non-metastasizing BSp73AS cells [41] was confirmed in numerous studies in human and animal models [ref. in 42]. The central role of CD44v in metastasis formation was confirmed by a knockdown of CD44v4-v7 (ASML-CD44v^{kd}) in ASML cells that poorly metastasize [43]. As the metastatic process essentially depends on the cross talk between tumor cells and the host and exosomes being suggested to be the most important intracellular communicators, we speculated that ASML^{wt} exosomes might account for the metastatic spread. Controlling this hypothesis was facilitated by the peculiarity of ASML cells not to grow locally after subcutaneous injection and to form metastases selectively in lymph nodes and lung [39]. Thus, if ASML exosomes contribute to premetastatic organ preparation, ASML-CD44v^{kd} cells that also do not grow locally should regain metastatic capacity after preparing the host with ASML^{wt} exosomes. Indeed, poorly metastasizing ASML-CD44v^{kd} cells regain metastatic capacity, when rats are pretreated with conditioned medium (CM) of ASML^{wt} cells. The essential contribution of exosomes was supported by the finding that exosome-depleted CM (CM^{-exo}) exerted no metastasis-promoting effect. Furthermore, compared to ASML^{wt} exosomes, ASML-CD44v^{kd} exosomes exerted a weaker effect [6]. To obtain hints toward the weaker effect of ASML-CD44v^{kd} *versus* ASML^{wt} exosomes, we explored the impact of metastasis-promoting CD44v6 on the exosomal mRNA, miRNA, and protein profiles and progressed toward elucidating how tumor exosomes modulate premetastatic organs using lymph node stroma cells (LnStr) and lung fibroblasts (LuFb) as targets.

Materials and Methods

Cell Lines

ASML^{wt} cells derive from the metastasizing variant of a spontaneously arisen rat pancreatic adenocarcinoma in the BDX rat strain. Subcutaneously implanted ASML cells do not grow locally and metastasize exclusively to lymph nodes and lung [39]. ASML-CD44v^{kd} cells do not also grow locally. They metastasize with a strong delay to draining lymph nodes and do not settle in the lung [43]. A rat aortic

endothelial cell line (EC) and a fibroblast line (LuFb) derived from the lung of BDX rats spontaneously immortalized. These lines as well as human embryo renal cortical cells (HEK293) and LnStr (B12) [44] were maintained in RPMI 1640/10% fetal calf serum, supplemented for ASML-CD44v^{kd} cells with 750 µg/ml G418.

Antibodies

For antibodies, see Table W1.

Exosome Preparation

Cells were cultured (48 hours) in serum-free medium. Cleared supernatants (2 × 10 minutes, 500g; 1 × 20 minutes, 2000g; 1 × 30 minutes, 10,000g) were centrifuged (90 minutes, 100,000g) and washed [phosphate-buffered saline (PBS), 90 minutes, 100,000g]. The supernatant after the last centrifugation was collected as CM^{-exo}. It was concentrated and, after protein determination, adjusted to 200 µg/25 µl for intrafootpad (ifp) injection. The pellet was resuspended (10 ml of PBS), layered on 10 ml of 40% sucrose, and centrifuged (90 minutes, 100,000g). The top layer was removed; the sucrose layer was diluted with PBS and centrifuged (90 minutes, 100,000g). Where indicated, exosomes were rhodamine–N-(lissamine rhodamine *B sulfonyl*) phosphatidyl ethanolamine (DHPE)– or SP-Dio$_{18}$(3)– labeled (Invitrogen, Karlsruhe, Germany). Exosomes were directly labeled (30 minutes, 4°C) before sucrose gradient centrifugation and washed twice (90 minutes, 100,000g). Relative fluorescence intensity was adjusted to rhodamine-DHPE or SP-Dio$_{18}$(3) standards.

mRNA and miRNA

After RNAse treatment, exosomal and cellular mRNA/miRNA were extracted using TRI reagent according to recommendation (Sigma, Munich, Germany).

Microarray mRNA Analysis

Expression levels of 22,523 rat transcripts of two independent preparations of ASML^{wt} and ASML-CD44v^{kd} exosomes and cells and of untreated and ASML^{wt}- or ASML-CD44v^{kd} exosome–treated LnStr cells were analyzed in duplicates or triplicates using Ilumina and SurePrintG3Rat-GE-8x60K microarray. Analyses, normalization, and statistics (Chipster analysis and Agilent annotation) were performed at the Core Facility, German Cancer Research Center. Cellular and exosomal samples were normalized independently. Transcripts with at least double signal intensity over background, bead standard error differences > 12, and P value < .05 were included (http://www.ncbi.nlm.nih.gov/geo/query/acc.cgi?acc=GSE34739). RNA was analyzed according to function clustering (http://www.pantherdb.org).

Microarray miRNA Analysis

miRNA analysis of ASML^{wt} and ASML-CD44v^{kd} exosomes and cells (Core Facility, European Molecular Biology Laboratories, Heidelberg, Germany) used the miRCURY LNA microRNA ver11.0-hsa,mmu, rno or the Agilent microRNA microarray evaluating quadruplicates of two independent preparation (http://www.ncbi.nlm.nih.gov/geo/query/acc.cgi?acc=GSE34739). Mean values of normalized data (Agilent Feature Extraction Software) were compared. Differentially regulated miRNA were defined as those with more than two-fold changes in signal strength. The miRNA database (http://www.microrna.org) and the target scan database (http://www.targetscan.org) were used to predict potential miRNA targets and for correlating downregulated mRNA in exosome-treated LnStr with exosomal miRNA.

Reverse Transcription and Quantitative Reverse Transcription–Polymerase Chain Reaction

Reverse transcription (RT) reactions contained RNA samples including purified total RNA, cell lysate, or heat-treated cells, 50 nM stem loop reverse transcriptase primer (Applied Biosystems, Darmstadt, Germany), 1× reverse transcriptase buffer (Applied Biosystems), 0.25 mM each of deoxyribonucleoside triphosphates (dNTPs), 3.33 U/μl Multi-Scribe reverse transcriptase (Applied Biosystems), and 0.25 U/μl RNase inhibitor (Applied Biosystems). The 7.5-μl reactions were incubated in an Applied Biosystems 9700 Thermocycler in a 96- or 384-well plate for 30 minutes at 16°C, 30 minutes at 42°C, and 5 minutes at 85°C and then held at 4°C. All reverse transcriptase reactions, including no template controls and reverse transcriptase minus controls, were run in duplicate.

Real-time polymerase chain reaction (PCR) was performed using a standard TaqMan PCR kit protocol on an Applied Biosystems 7900HT Sequence Detection System (Applied Biosystems). The 10-μl PCR included 0.67 μl of reverse transcriptase product, 1× TaqMan Universal PCR Master Mix (Applied Biosystems), 0.2 μM TaqMan probe, 1.5 μM forward primer, and 0.7 μM reverse primer. The reactions were incubated in a 384-well plate at 95°C for 10 minutes, followed by 40 cycles of 95°C for 15 seconds and 60°C for 1 minute. All reactions were run in triplicate. Glyceraldehyde phosphate dehydrogenase (GAPDH) served as internal control for mRNA and 4.5SRNA was used as internal control for miRNA. The threshold cycle (C_T) is defined as the fractional cycle number at which the fluorescence passes the fixed threshold. TaqMan C_T values were converted into absolute copy numbers using a standard curve from synthetic lin-4 miRNA. Statistical analysis was done by the ΔC_T method [$^\Delta C_T = C_T$ test gene – C_T endogenous control; $^{\Delta\Delta} C_T = {}^\Delta C_T$ sample – $^\Delta C_T$ calibrator (untreated LnStr)], where relative quantification/fold change compared to the calibrator = $2^{-\Delta\Delta C_T}$.

miRNA Transfection

LnStr and HEK293 cells, seeded in antibiotic-free medium (24 hours), were transfected with 20 nM [quantitative RT-PCR (qRT-PCR)] or 10 nM (luciferase reporter assay) miRNA mimic (Qiagen, Hilden, Germany) using Lipofectamine 2000. After 48 hours, mRNA regulation was evaluated by qRT-PCR and/or was verified by flow cytometry (protein level) or used for luciferase reporter assay.

3′UTR Reporter Assay

miRNAs that could bind in the 3′UTR of MAL and cadherin-17 (cdh17) mRNAs were searched according to http://www.microrna.org. Those showing a good mirSVR score (lower than –0.1) and detected in exosomes were selected. The 3′UTR regions were cloned by PCR from genomic LnStr DNA (primers: Table W2). PCR products were cloned into the dual-luciferase pmiRGlo vector, downstream of firefly luciferase using Pme1 and Xba1 restriction sites. After ligation and bacterial transformation, positive clones (sequenced) were used for HEK293 transfection. HEK293 cells were transfected with cloned miRNA binding sites for miR-300-5p or of the 3′UTRs of MAL and cdh17 using HiPerFect for reverse transfection in 96-well plates. Briefly, miRNA mimics (10 nM; Qiagen) without or with 80 ng of the reporter plasmid was spotted in a well of 96-well flat-bottom plates. Thereafter, HiPerFect reagent (1 μl, diluted in 25 μl of serum-free medium) was added to the miRNA/DNA and mixed by pipetting. After an incubation time of 10 minutes, 4×10^5 cells in Iscoves/10% fetal calf serum were added. The cells were maintained under normal growth condition for 48 hours. The Dual-Luciferase Reporter Assay Kit (Promega, Mannheim, Germany) was performed following the manufacturer's instruction. Cells were lysed in 20 μl of Dual-Glo reagent (15 minutes, reverse transcriptase); the lysate was added to 100 μl of the same reagent in a white 96-well plate (Promega), and the firefly luciferase was measured using FLUOstar OPTIMA luminometer (BMG LABTECH, Offenburg, Germany), followed by measurement of Renilla luciferase, which was used for normalization of transfection efficiency.

In Vitro Translation

Exosomal RNA (10 μg) in water was mixed with 1.25 μl of 20× translation mix (Retic Lysate IVT Kit), 1 μl of ^{35}S-methionine, and 17 μl of Retic lysate, adjusted to 25 μl with nuclease-free water. After vortexing and centrifugation, the reaction mix at the bottom of the tube was incubated for 90 minutes in a 30°C water bath and for 10 minutes with 2.5 μl of RNaseA; 10 μl of the complete reaction was mixed with an equal volume of 2× sodium dodecyl sulfate sample buffer and incubated for 5 minutes at 95°C. After centrifugation, samples were collected from the bottom and allowed to cool to room temperature. Samples were loaded on a 12% sodium dodecyl sulfate–gel. After electrophoresis, proteins were fixed (45% methanol and 10% acetic acid, 5 minutes, gentle agitation) and dried. Dried gels were exposed at –70°C for 48 hours to X-ray films using an intensifying screen and photographed.

Flow Cytometry

Flow cytometry for cells followed routine procedures. Where indicated, cells were fixed and permeabilized and/or stripped (two washes in PBS/HCl, pH 2.5). Exosomes (10–15 μg) were incubated with 1 μl of aldehyde-sulfate latex beads (4 μm) (Invitrogen) in PBS/1% BSA (90 minutes, 20°C, shaking). After centrifugation, free binding sites on the beads were blocked by incubation with 100 mM glycine in PBS (1 hour). After washing two times with PBS/1% BSA, exosome-coated beads (corresponding to 1 μl beads/well) are distributed in 96-well plates. Staining with primary and secondary dye-labeled antibodies follows the protocol for cell staining. For analyzing exosome uptake, cells were incubated with DHPE-labeled exosomes, washed, and stripped. Samples were analyzed in a FACSCalibur using the CellQuest program.

Zymography

CM of LnStr (1×10^6), starved for 24 hours, was centrifuged (15 minutes, 15,000g). Aliquots of supernatant were incubated with Laemmli buffer (15 minutes, 37°C) and separated in a 10% acrylamide gel containing 1 mg/ml gelatin. After washing (2.5% Triton), gels were incubated in developing buffer (37°C, 48 hours) and stained with Coomassie Blue.

In Vivo Assays

Rats (three per group) receiving 200 μg of SP-Dio$_{18}$(3)–labeled exosomes in 25 μl of RPMI 1640, ifp, were sacrificed after 24 to 72 hours. Rats (three per group) receiving exosomes in RPMI 1640 or 20-fold concentrated CM^{-exo} of ASML^{wt} or ASML-CD44v^{kd} cells, ifp, were sacrificed after 48 hours. Popliteal lymph nodes were excised and dispersed to evaluate exosome uptake by flow cytometry. The experiment was government-approved (Baden-Wuerttemberg, Germany).

Statistical Analysis

All *in vitro* assays were run in triplicates and repeated at least three times. *P* values < .05 (two-tailed Student's *t* test, analysis of variance) were considered significant. The mRNA and miRNA microarray analyses were performed with two independent samples, each run in duplicate or triplicate (mRNA) or quadruplicate (miRNA) and contained 60 (mRNA) or >30 (miRNA) negative controls. As the duplicate/triplicate (mRNA) and quadruplicate (miRNA) samples frequently revealed *P* values < .05 with as low a variation in the signal strength as 1.2, mean values of the duplicates/quadruplicates of the two independent performed microarray analyses are presented throughout, where it should be noted that in the absolute ranking the individual mRNA/miRNA were very close and the few samples where this has not been the case were excluded. Nonetheless, as the total signal strength between the two microarrays differed, *P* values < .05 were rare and are only occasionally included. Instead, we indicate more than two-fold differences (which is five times the level to reach significant *P* values within the individual microarray analysis).

Results

ASML cells, not forming a local tumor, metastasize through the lymphatics to the lung [39], indicating an essential requirement of lymph node or lung environment for growth. This feature makes ASML cells ideal candidates for defining a tumor's impact on premetastatic niche preparation. In a previous work indicating that exosomes are essential [6], we here characterized ASML[wt] exosomes and defined their impact on LnStr and LuFb. The comparison with ASML-CD44v[kd] exosomes aimed for hints toward their lower efficacy.

In Vivo *and* In Vitro *Exosome Binding and Uptake*

As a prerequisite for *in vivo* activity, we controlled that tumor exosomes reach the premetastatic organ from the distant site of the primary tumor. Ifp-injected ASML[wt] exosomes were recovered in the popliteal node after 24 to 72 hours. ASML[wt] exosome and, far more pronounced, ASML-CD44v[kd] exosome recovery was significantly increased, when supported by ASML[wt]-CM[−exo]. The ASML-CD44v[kd]-CM[−exo] hardly supported exosome traffic toward the popliteal node (Figure 1, *A–C*).

ASML exosomes are taken up by leukocytes [45] and stroma cells. As ASML cells metastasize exclusively through the lymphatic system, we chose LnStr and LuFb as targets to explore *in vitro* the impact of tumor exosomes. ASML[wt] exosomes bind more rapidly than ASML-CD44v[kd] exosomes to LnStr and LuFb. Both exosomes bind less efficiently to ECs, included as control (Figure 1, *D* and *E*). Bound exosomes are taken up by their targets, as seen in the sagittal sections of exosome-treated LnStr and LuFb (Figure 1*E*) and confirmed by exposing LnStr and LuFb to two acid washes (pH 2.5; stripping), which remove bound without affecting integrated exosomes. ASML[wt] exosome uptake proceeds more rapidly than ASML-CD44v[kd] exosome uptake (Figure 1, *F* and *G*).

Thus, ASML exosomes reach the premetastatic organ *in vivo* and are *in vitro* taken up by LnStr and LuFb. The CD44v[kd] has some, not yet, explored impact on the efficacy of exosome binding and uptake.

ASML Exosomal mRNA and miRNA

Having demonstrated that ASML[wt] and ASML-CD44v[kd] exosomes are taken up by host stroma cells, though with distinct efficacy, we focused on the potential contribution of CD44v to protein, mRNA,

and miRNA recruitment into exosomes, where mRNA and miRNA are claimed to be selectively recruited into MVB/exosomes [20–23,26].

The RatRef-12 expression BeadChip array (23,365 transcripts) revealed <1500 mRNAs in ASML[wt] and ASML-CD44v[kd] exosomes (Table W3) but >8000 mRNAs in ASML cells (Table W4), indicating a restricted mRNA uptake by exosomes. To strengthen the assumption, we compared the relative abundance of exosomal *versus* cellular mRNA. Although the overall distribution of function-assigned groups of mRNA was similar in ASML[wt] and ASML-CD44v[kd] exosomes and cells and also LnStr (data not shown), the relative abundance of exosomal *versus* cellular mRNA differed. From 116 mRNAs highly recovered in ASML[wt] exosomes, the relative recovery of >90 mRNAs differed more than two-fold in ASML[wt] cells. Similar findings accounted for the comparison of ASML-CD44v[kd] exosomes *versus* cells (Table W5 and Figure W1). An elegant study by Eldh et al. [46] demonstrated that the mRNA isolation kit that was used provides a poor yield of exosomal mRNA. Nonetheless, several mRNAs were clearly enriched in exosomes. However, according to the above-mentioned study, we cannot exclude that an even higher number of mRNA is enriched in exosomes. As some mRNAs were enriched in ASML[wt] as well as ASML-CD44v[kd] exosomes, we next asked whether CD44v has an impact on mRNA recruitment into MVB. To obtain a hint, we evaluated the mRNA in ASML[wt] cells *versus* ASML-CD44v[kd] cells and compared these differences in cellular mRNA with those seen in exosomes. Should CD44v contribute to mRNA recruitment into exosomes, one would expect a significantly higher number of distinctly recovered mRNA in ASML[wt] exosomes than in cells. This has not been the case. Taking the 50 mRNAs with the highest signal intensity, two exosomal *versus* three cellular mRNA differed more than two-fold depending on CD44v (Figure 2, *A* and *B*). Taking 2390 defined mRNAs in ASML[wt] exosomes with a signal strength of >1000, only 74 (3.1%) differed more than two-fold in ASML-CD44v[kd] exosomes. Furthermore, when analyzing the cellular-to-exosomal mRNA ratio for 14 mRNAs (signal strength > 400), where the exosomal ASML[wt] mRNA was at least two-fold higher than the ASML-CD44v[kd] mRNA, no correlation to a higher ASML[wt] than ASML-CD44v[kd] cellular mRNA ratio was detected. Accordingly, no inverse correlation of the cellular mRNA was detected for ASML-CD44v[kd] exosomes containing a higher mRNA level than ASML[wt] exosomes (Figure W2).

However, CD44v could still contribute to the protein composition of exosomes. To answer this question, we selected cellular mRNA of proteins abundantly expressed in exosomes (http://www.exocarta.org). From 164 selected proteins with a cellular mRNA signal > 1000 in ASML[wt] cells, 25% showed a more than two-fold change in signal strength in ASML-CD44v[kd] cells, which is shown for the 50 mRNAs with the highest signals (Figure 2*C*) and as scatter for the first 100 mRNAs (Figure W3). The impact of CD44v on these mRNAs is reflected at the cellular and exosomal protein levels demonstrated by flow cytometry for CD24 and claudin-4 that expression is reduced in ASML-CD44v[kd] cells and exosomes, whereas caveolin-1 and CD81 expression are higher in ASML-CD44v[kd] than in ASML[wt] cells and exosomes (Figure 2*D*).

A rather low number (89–98) of miRNA were recovered in ASML[wt] and ASML-CD44v[kd] exosomes and cells (Table W6 and Figure W4: most abundant miRNA). With a >1000 signal strength cutoff, 21 cellular and 50 exosomal miRNAs differed more than two-fold between ASML[wt] and ASML-CD44v[kd] cells/exosomes (Figure W5). The distinct recovery in ASML[wt] *versus* ASML-CD44v[kd] cells indicates a direct or indirect contribution of CD44v6 to miRNA
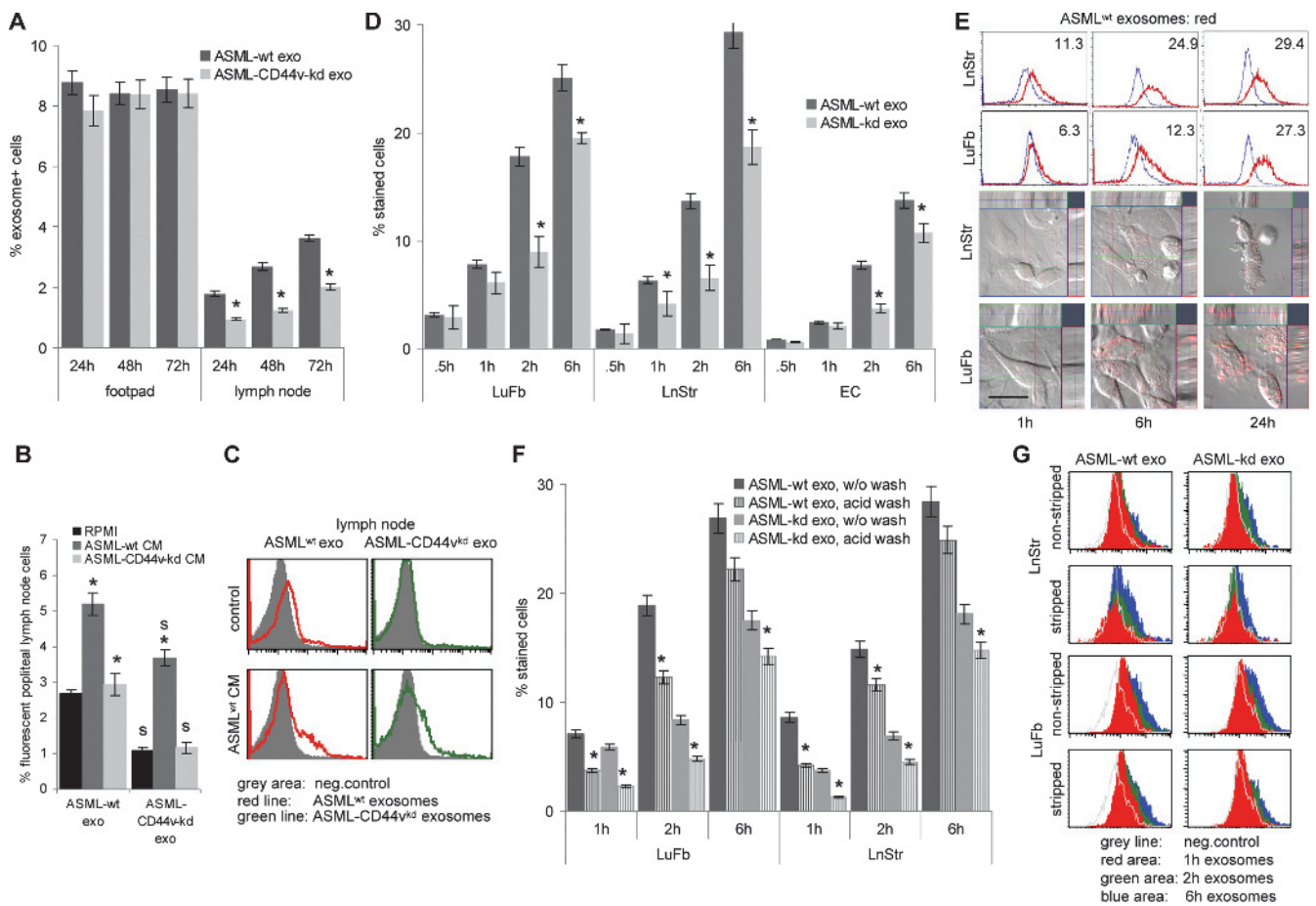
Figure 1. Exosome binding and uptake by non-transformed cells *in vivo* and *in vitro*. (A–C) Dye-labeled ASML^{wt} and ASML-CD44v^{kd} exosomes in RPMI 1640, ASML^{wt}, or ASML-CD44v^{kd}-CM^{-exo} were injected ifp. Rats were sacrificed after 24 to 72 hours; the injection site and the popliteal node were excised and dispersed, and fluorescent exosome uptake was evaluated in single-cell suspensions by flow cytometry counting 100,000 cells for each organ in triplicate. (A) Mean values ± SD (triplicates, three rats) of fluorescent cells; significant differences between ASML^{wt} and ASML-CD44v^{kd} exosomes: *. (B) Mean values ± SD (triplicates, three rats) of fluorescent cells; significant differences in the presence of CM^{-exo}: *, and between ASML^{wt}- and ASML-CD44v^{kd} exosomes: **s**. (C) representative example. (D–G) LuFb, LnStr, and EC were incubated with dye-labeled ASML^{wt} and ASML-CD44v^{kd} exosomes (30 μg/ml) for the indicated times. (D) After washing, the percent fluorescent cells (mean ± SD, triplicates) were evaluated by flow cytometry; significant differences between the percentage of cells that bind/take up ASML^{wt} *versus* ASML-CD44v^{kd} exosomes: *. (E) Representative example of exosome uptake as evaluated by flow cytometry and confocal microscopy. Overlays of light field and red fluorescence including sagittal sections are shown (scale bar, 5 μm). (F and G) After 1, 2, and 6 hours, bound exosomes were removed by two acid washes (stripping), evaluating remaining fluorescence as above. (F) The percentage of stained cells (mean ± SD of triplicates); significant differences between the percentage of cells that bound/took up *versus* the percentage of cells that took up ASML^{wt} or ASML-CD44v^{kd} exosomes: *. (G) Representative examples are shown. Experiments in D to G were repeated at least three times revealing comparable results. ASML^{wt} and ASML-CD44v^{kd} exosomes reach the draining node; the efficacy can be improved by ASML^{wt}-CM. ASML exosomes bind more readily to LuFb and LnStr than to EC. Binding and uptake of ASML-CD44v^{kd} exosomes are less efficient and delayed compared to ASML^{wt} exosomes. It should be mentioned that the percentage of exosome uptake will be underestimated, as the signal strength of a single or few exosomes will be below the detection limit.

transcription or posttranscriptional regulation. Should CD44v, in addition, actively contribute to miRNA recruitment into MVB/exosomes, one would expect that the ratio of cellular to exosomal miRNA differs in dependence on CD44v expression. This has not been the case. With very few exceptions, the ratio of ASML^{wt} to ASML-CD44v^{kd} miRNA in cells did not differ significantly from that in exosomes and only one miRNA (miR-30e) was opposingly recruited into ASML^{wt} *versus* ASML-CD44v^{kd} exosomes (Figure 3).

Taken together, exosomes collect a limited number of mRNA and miRNA. The abundant differences in the mRNA of ASML^{wt} *versus* ASML-CD44v^{kd} cells argue for CD44v or associated molecules being

engaged in gene transcription/regulation. This includes genes whose protein products are enriched in exosomes [6,45, Figure W3, and unpublished findings]. However, differences at the cellular mRNA level between ASML^{wt} and ASML-CD44v^{kd} cells are closely reflected by differences in exosomes. Thus, CD44v seemingly does not actively contribute to MVB formation and has, if at all, only a minor impact on mRNA recruitment into MVB.

Having characterized ASML^{wt} and ASML-CD44v^{kd} exosomal mRNA and miRNA, we asked whether they have any impact on exosome targets, where we focused on the general principle rather than on the differences between ASML^{wt} *versus* ASML-CD44v^{kd} exosomes.
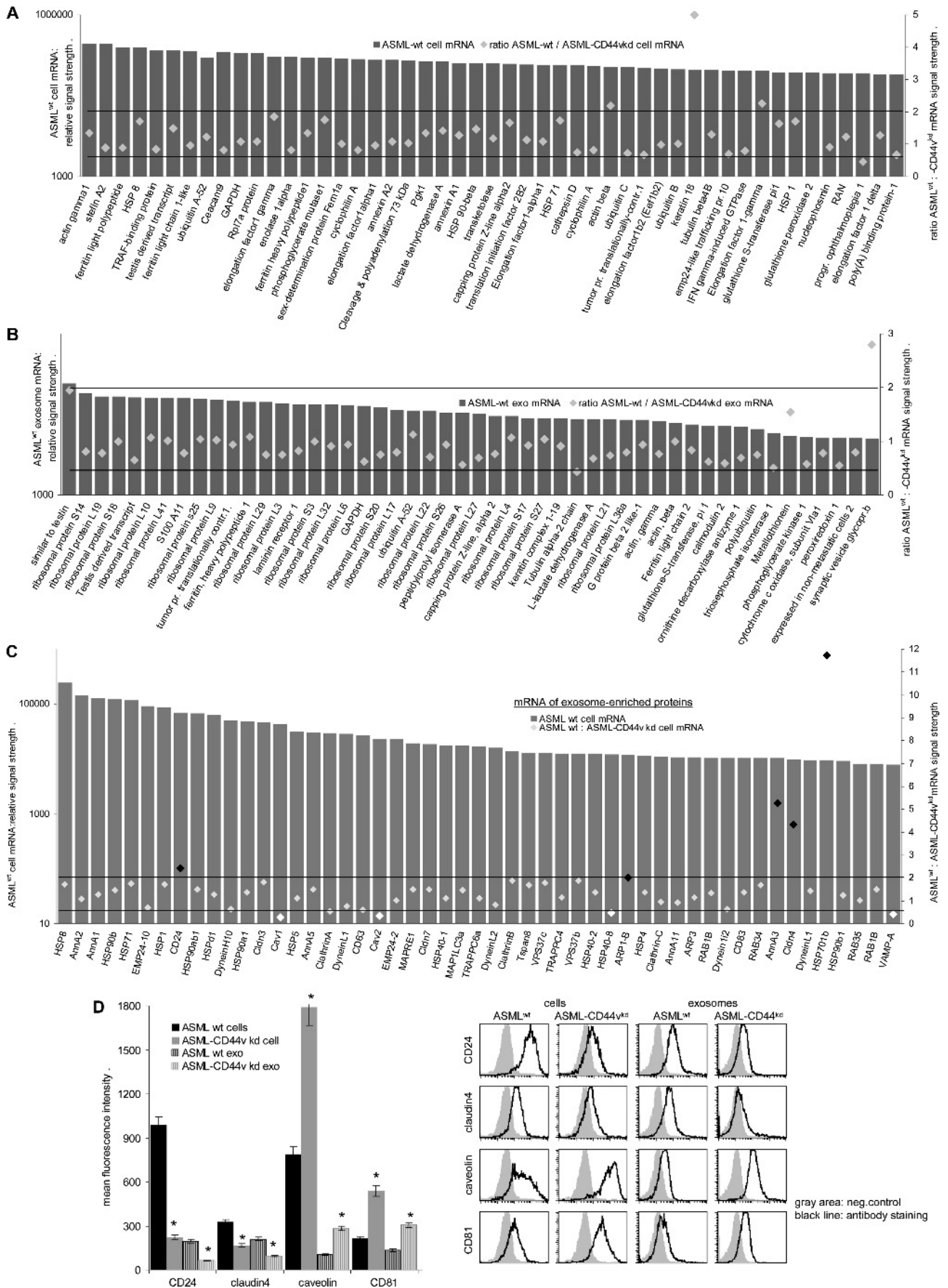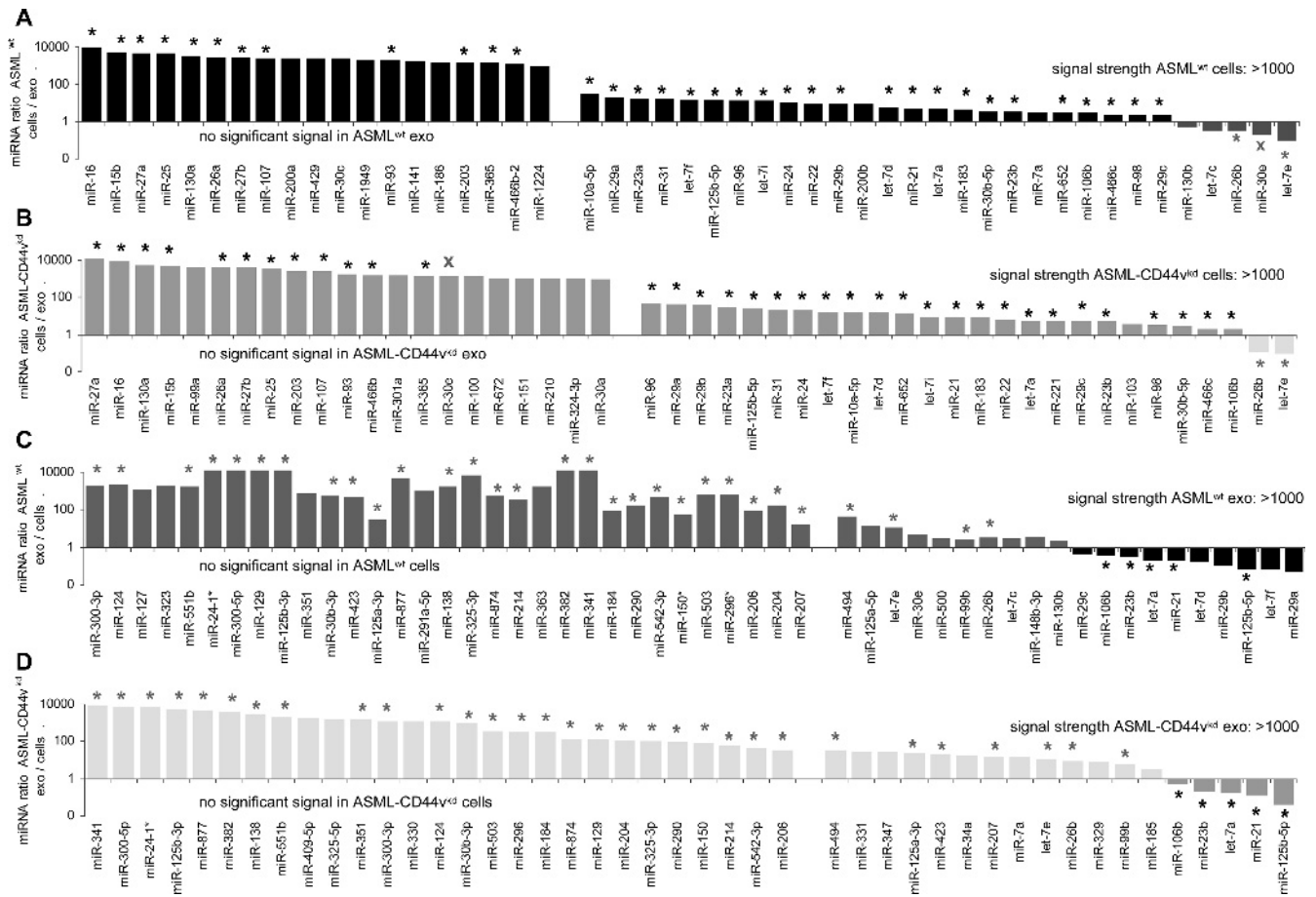
Figure 3. miRNA ratio in ASML cells *versus* exosomes. (A–D) The miRNAs (signal strength > 1000, mean of quadruplicates of two microarray analyses) are depicted, where the ratio reveals a more than two-fold change in (A) ASML^wt and (B) ASML-CD44v^kd cells to exosomes and in (C) ASML^wt and (D) ASML-CD44v^kd exosomes to cells; alike regulation in ASML^wt and ASML-CD44v^kd cells *versus* exosomes: *; opposing up-regulation or down-regulation: X. The miRNA profile of exosomes differs strikingly from that of cells, a considerable number of cellular miRNA being not detected in exosomes and *vice versa*. Instead, there are minor differences in ASML^wt *versus* ASML-CD44v^kd cells and exosomes, indicating that CD44v might not be engaged in miRNA recruitment into MVB.

ASML Exosome mRNA and miRNA Are Transferred into LnStr

We first reaffirmed for selected mRNA and miRNA the transfer into target cells. For mRNA, C4.4A was chosen, as C4.4A is not detected in LnStr. Instead, it was recovered after co-culture with exosomes (Figure 4*A*). Though exosomal mRNA integrity was confirmed by

in vitro translation (data not shown), *in vivo* translation of C4.4A was not detected. As revealed by double fluorescence analysis of LnStr co-cultured with dye-labeled exosomes, upregulated expression/translation of other more abundant exosomal mRNA, like CD24 and cyclin D1, was detected but was not restricted to LnStr that had taken up ASML^wt exosomes (Figure 4*B*).

Figure 2. ASML^wt and ASML-CD44v^kd cellular and exosomal mRNAs. (A and B) Examples of 50 defined mRNAs with the highest signal strength in ASML^wt cells and exosomes and fold changes in ASML-CD44v^kd cells and exosomes. (C) mRNA signals in ASML^wt cells and fold change in ASML-CD44v^kd cells for 50 proteins known to be highly recovered in exosomes. (A–C) Mean values were derived from duplicates/triplicates in two independent microarray analyses, where it should be noted that in both arrays the absolute ranking of individual mRNA was very high, at least for those with a signal strength of >2000. However, whereas by calculating *P* values from the duplicates/triplicates of the individual array 1.2-fold differences mostly were significant, the absolute signal strength varied between the two arrays such that *P* values < .05 were mostly not reached. For these reasons, we indicate more than two-fold differences that are generally accepted as non-random. (D) For selected mRNA, protein recovery was evaluated in ASML^wt and ASML-CD44v^kd cells and exosomes by flow cytometry. Representative examples and mean ± SD (triplicates) of staining intensity in ASML^wt and ASML-CD44v^kd cells and exosomes are shown. Significant differences between ASML^wt *versus* ASML-CD44v^kd cells and exosomes: *. (D) The experiment was repeated three times revealing comparable results. Exosomes contain a limited number of mRNA. However, more than two-fold differences in ASML^wt *versus* ASML-CD44v^kd exosomal mRNA are rare and not selectively recovered in exosomes, suggesting that CD44v is unlikely to be directly involved in mRNA recruitment into MVB. Conversely, CD44v or associated molecules affect transcription of several genes, including transcription of genes/expression of proteins, which are constitutive exosome components. Thereby, CD44v contributes to the protein and mRNA profile of exosomes.
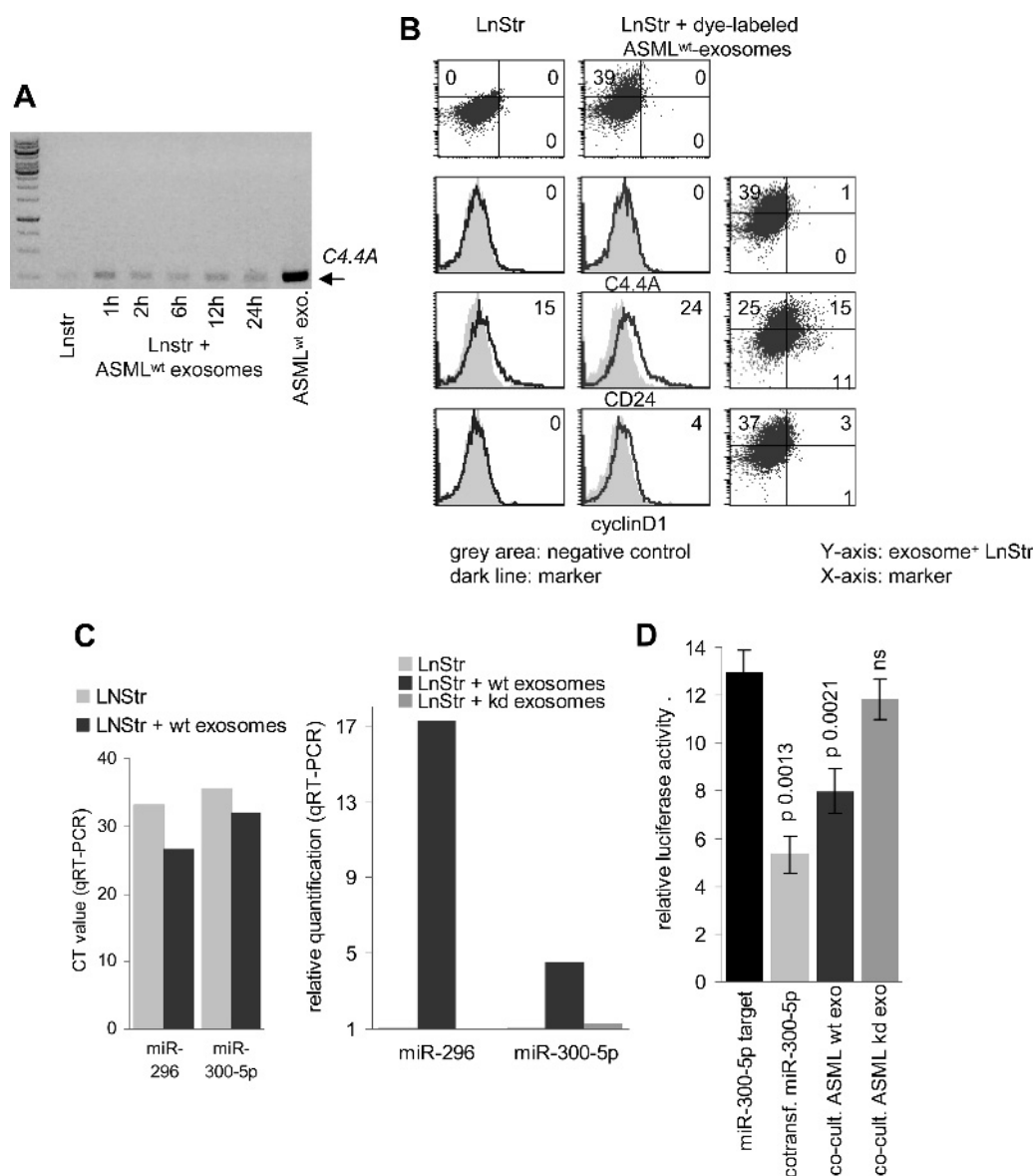
Figure 4. Recovery of exosomal mRNA and miRNA in target cells. (A) LnStr cells were co-cultured with ASML^{wt} exosomes. After 1 to 24 hours, mRNA was extracted, reverse transcribed, amplified with C4.4A-specific primers by RT-PCR, and separated by agarose gel. (B) LnStr were co-cultured (6 hours) with DHPE-labeled ASML^{wt} exosomes and were stained with anti-C4.4A (C4.4), anti-CD24, and anti–cyclin D1 after washing, fixation, and permeabilization. Flow cytometry of untreated and ASML^{wt} exosome–treated LnStr (overlay with negative control and double fluorescence: DHPE-labeled exosomes and marker) is shown. (C) After 48 hours of co-culture, LnStr RNA was extracted, reverse transcribed, and amplified using universal reverse primer and miR-specific forward primer with stem loop primers for miR-296 and miR-300-5p. C_T and relative quantification values (mean of three replicate samples with SD < 0.25, indicating reliability according to the software program for ΔC_T) in untreated *versus* ASML^{wt} and ASML-CD44v^{kd} exosome–treated LnStr are shown. (D) HEK293 cells were transfected with the dual-luciferase pmiRGlo vector containing a miR-300-5p binding site and were co-transfected with miR-300-5p (10 nM) or co-cultured with ASML^{wt} or ASML-CD44v^{kd} exosomes (20 µg). Firefly and, for normalization, Renilla luciferase activity was evaluated after 48 hours in a FLUOstar OPTIMA luminometer. Relative luciferase activity (mean ± SD, triplicates) and P values for miR-300-5p, ASML^{wt} and ASML-CD44v^{kd} exosomes are shown. (C and D) Experiments were repeated three times revealing comparable results. Exosomal mRNA and miRNA are transferred. *In vivo* mRNA translation was hardly detectable and endogenous transcription/translation cannot be safely excluded. Transferred exosomal miRNA is active.

miRNA transfer was confirmed for miR-300-5p and miR-296, abundant in ASML^{wt} exosomes and found to be 4.5-fold and 17.3-fold increased in ASML^{wt}-exosome–treated compared to untreated LnStr. Notably, after co-culture with ASML-CD44v^{kd} exosomes that express significantly less miR-300-5p, no significant increase in miR-300-5p was seen in LnStr (Figure 4C). Functional-ity of the transferred exosomal miRNA was controlled by a reporter assay with a dual-luciferase pmiRGlo vector with a binding site for miR-300-5p downstream of the firefly luciferase gene. Luciferase activity in HEK293 cells co-transfected with miR-300-5p mimic, but also and importantly, when co-incubated with ASML^{wt} exosomes was significantly decreased. A similar effect was not observed

after co-culture with low-level miR-300-5p expressing ASML-CD44v^{kd} exosomes (Figure 4D).

Taken together, exosomal mRNA and miRNA are transferred into target cells. Exosomal miRNA is function-competent. Exosomal mRNA becomes translated, but we could not unequivocally detect the exosomal mRNA translation product, which might be due to the low amount of exosomal mRNA.

The Impact of Exosomal mRNA on LnStr and LuFb

Having demonstrated exosomal mRNA and miRNA transfer, we searched for altered mRNA recovery in LnStr after co-culture with exosomes.

The signal strength of 38 mRNAs and 20 mRNAs with moderate to high expression in LnStr increased more than two-fold after co-culture with ASML^{wt} or ASML-CD44v^{kd} exosomes, respectively
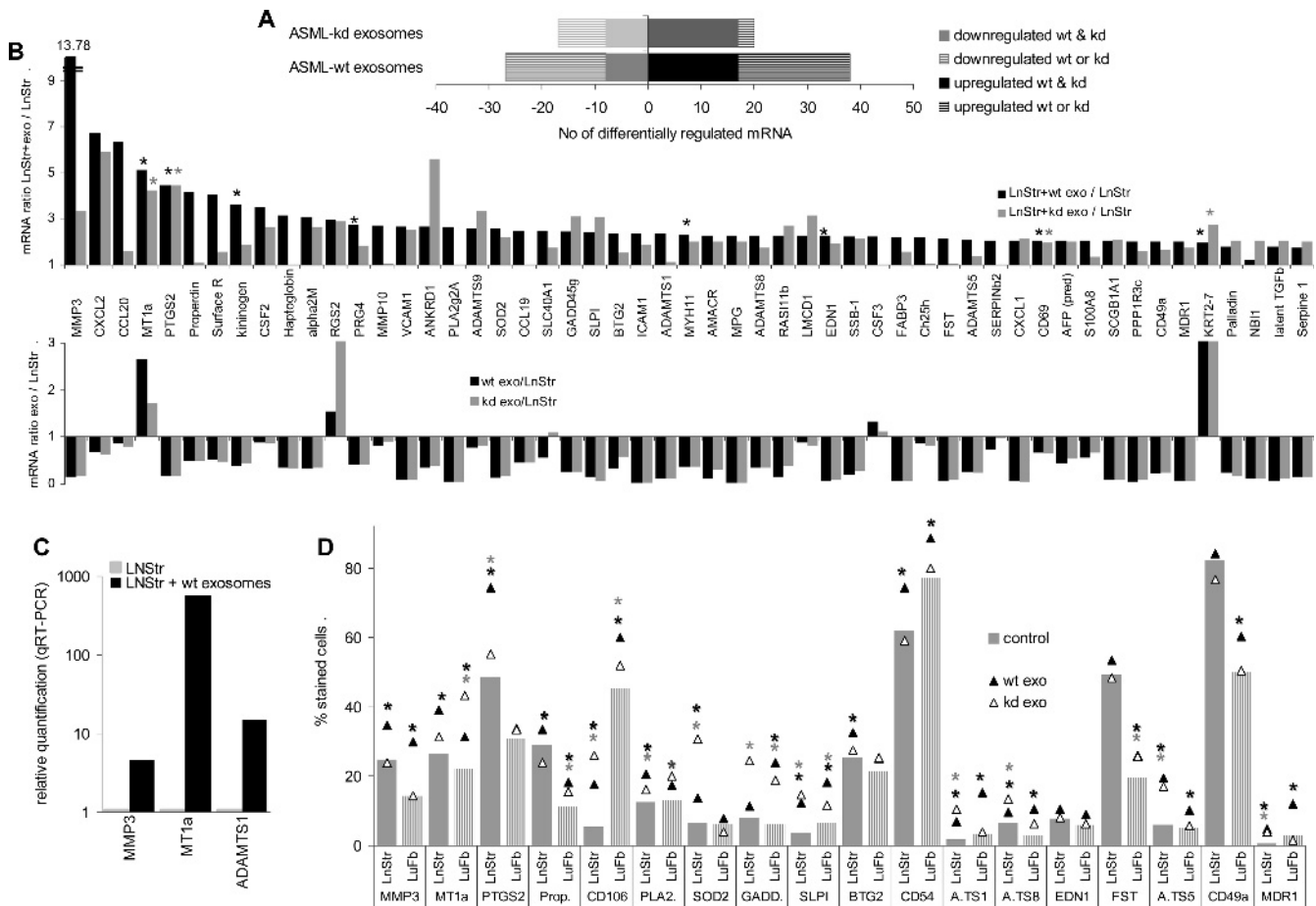
Figure 5. Impact of ASML^{wt} and ASML-CD44v^{kd} exosomes on mRNA and protein expression in LnStr and LuFb. (A–D) LnStr and LuFb were co-cultured for 48 hours with ASML^{wt} and ASML-CD44v^{kd} exosomes. (A and B) Cells were harvested, washed, and lysed and mRNA was extracted and analyzed (Ilumina and SurePrintG3Rat-GE-8x60K microarray). (A) Number of LnStr mRNA with a more than two-fold change after co-culture with ASML^{wt} or ASML-CD44v^{kd} exosomes. (B) mRNA in LnStr that are more than two-fold upregulated after co-culture with exosomes and comparison of the relative mRNA amount in exosomes *versus* LnStr. (A and B) Mean values of duplicates, respectively, triplicates, of two independent microarray analyses. (B) Significant differences between LnStr and LnStr co-cultured with ASML exosomes: *. (C) Upregulated gene expression (selected examples) in LnStr co-cultured with exosomes was confirmed by qRT-PCR (mean of three replicate samples with SD < 0.25, indicating reliability according to the software program for ΔC_T) and (D) in LnStr and LuFb at the protein level by flow cytometry. The mean percentage of stained cells (triplicates) are shown; significant differences between untreated LnStr/LuFb and LnStr/LuFb co-cultured with ASML^{wt} exosomes: black *; significant differences between untreated LnStr/LuFb and LnStr/LuFb co-cultured with ASML-CD44v^{kd} exosomes: gray *. (C and D) Experiments were repeated three times revealing comparable results. Abbreviations: MMP3, matrix metalloproteinase 3; CXCL2, chemokine ligand 2; CCL20, chemokine ligand 20; MT1a, metallothionein; PTGS2, prostaglandin-endoperoxide synthase 2; alpha2M, alpha-2-macroglobulin; RGS2, regulator of G-protein signaling 2; PRG4, proteoglycan 4; VCAM1, vascular cell adhesion molecule–1/CD106; ANKRD1, ankyrin repeat domain 1; PLA2g2A, phospholipase A2 group 2A; SOD2, superoxide dismutase 2; CCL19, chemokine ligand 19; SLC40A1, solute carrier family 39; GADD45g, growth arrest and DNA-damage-inducible 45γ; SLPI, secretory leukocyte peptidase inhibitor; BTG2, B-cell translocation gene 2; ICAM1, intercellular adhesion molecule 1/CD54; MYH11, myosin heavy chain 11; AMACR, α-methylacyl-CoA racemase; MPG, matrix Gla protein; ADAMTS8, a disintegrin-like and metalloprotease with thrombospondin type 1, motif 8; RASl11b, RAS-like family 11 member B; EDN1, endothelin 1; SSB-1, SPRY domain-containing SOCS box protein SSB-1; FABP3, fatty acid binding protein 3; FST, follistatin; ADAMTS5, ADAMTS, motif 5; CXCL1, chemokine ligand 1; SCBG1A1, secretoglobin, family 1A, member 1; PPP1R3c, protein phosphatase 1, regulatory subunit 3C; CD49a, integrin α1; MDR1, ATP-binding cassette, subfamily B, member 1; KRT2-7, keratin complex 2; NBI1, neuroblastoma suppression of tumorigenicity; latent TGFβ, latent TGFβ binding protein.
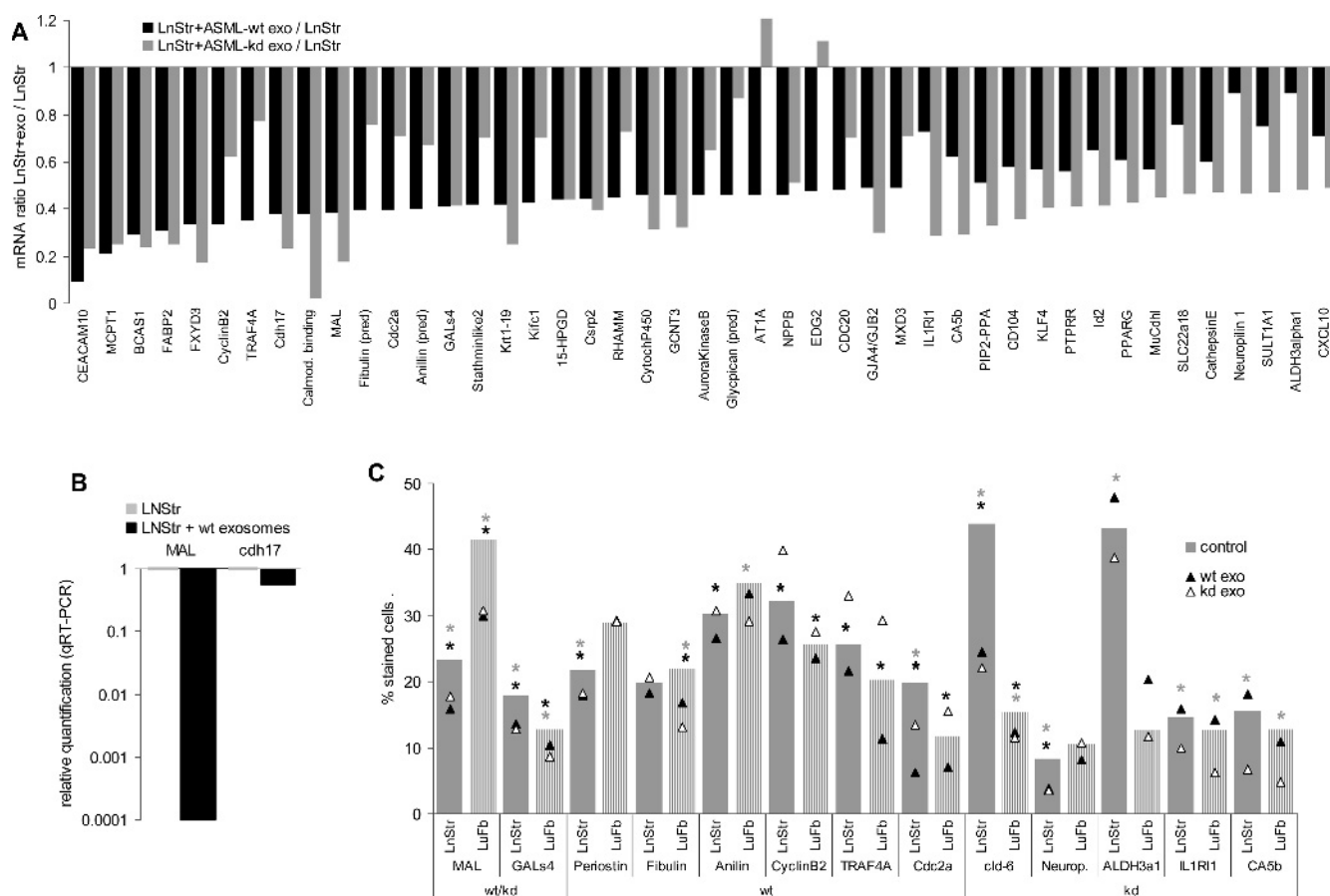
Figure 6. Reduced mRNA recovery and protein expression in LnStr and LuFb after co-culture with ASML[wt] and ASML-CD44v[kd] exosomes: mRNA analysis was performed as described in Figure 5. (A) mRNA whose expression was reduced in LnStr by more than two-fold after co-culture with exosomes. (B) Confirmation of mRNA down-regulation (selected examples) by qRT-PCR (mean of three replicate samples with SD < 0.25, indicating reliability according to the software program for ΔC_T) and (C) at the protein level in LnStr and LuFb by flow cytometry (mean percentage of stained cells, triplicates); examples are grouped according to reduced mRNA recovery after co-culture with ASML[wt] and ASML-CD44v[kd] or ASML[wt] or ASML-CD44v[kd] exosomes; significant differences between untreated LnStr/LuFb and LnStr/LuFb co-cultured with ASML[wt] exosomes: black *; significant differences between untreated LnStr/LuFb and LnStr/LuFb co-cultured with ASML-CD44v[kd] exosomes: gray *. (B and C) Experiments were repeated three times revealing comparable results. mRNA microarray analysis confirmed the strong impact of exosomes on mRNA recovery in target cells. Many effects were observed with ASML[wt] and ASML-CD44v[kd] exosomes, but distinct regulations, e.g., of cyclin B2, TRAF4, IL1RI1, and Id2 by ASML[wt] and ASML-CD44v[kd] exosomes were also observed. Abbreviations: CEACAM10, CEA-related cell adhesion molecule 10; MCPT1, mast cell protease; BCAS1, breast carcinoma amplified sequence; FABP2, fatty acid binding protein 2; FXYD3, FXYD domain-containing ion transporter regulator 3; TRAF4, TNF receptor–associated factor 4; cdh17, cadherin-17; MAL, myelin and lymphocyte protein; Cdc2a, cell division cycle 2 homolog A; GALs4, galactose binding soluble 4 lectin; Krt1-19, keratin complex 1, acidic, gene 19; Kifc1, kinesin family member C1; 15-HPGD, 15-hydroxyprostaglandin dehydrogenase; Csrp2, cysteine and glycine-rich protein 2; GCNT3, glucosaminyl (N-acetyl) transferase 3; AT1A, angiotensin II receptor 1; NPPb, natriuretic peptide precursor type B; EDG2, endothelial differentiation, lysophosphatidic acid G protein–coupled receptor 2; CDC20, cell division cycle 20 homolog; GJA4/GJB2, GAP junction membrane channel; MXD3, Max dimerization protein; IL1RI1, interleukin-1 receptor-like 1; CA5b, carbonic anhydrase VB; CD104, integrin β4; KLF4, Kruppel-like factor 4; PTPRR, protein tyrosine phosphatase, receptor type; Id2, inhibitor of DNA binding 2; PPARG, peroxisome proliferator–activated receptor gamma; MuCdhl, mucin and cadherin like; SLC22a18, tumor-suppressing subtransferable candidate 5; SULT1A1, sulfotransferase family 1A; ALDH3α1, aldehyde dehydrogenase family 3, member A1.

(Figure 5A). Increased mRNA signals were unexpected, as with few exceptions the signal strength in exosomes was lower than in LnStr (Figure 5B), and for 36 of the 38 mRNAs upregulated in ASML[wt] exosome–treated LnStr cells, the exosomal mRNA signal strength was low (<1000). Nonetheless, qRT-PCR confirmed matrix metalloproteinase 3 (MMP3), metallothionein (MT1a), and a disintegrin-like and metalloprotease with thrombospondin type 1 (ADAMTS1) up-regulation in LnStr after co-culture with ASML exosomes (Figure 5C). From 18 mRNAs, where expression was con-

trolled at the protein level, 14 were significantly upregulated in LnStr and 13 in LuFb after co-culture with ASML[wt] exosomes. Similar effects were observed after co-culture with ASML-CD44v[kd] exosomes (Figure 5D).

In view of the low levels of exosomal mRNA and the inefficient translation in host cells, it becomes unlikely that altered mRNA/protein expression in exosome-treated targets derives from transferred exosomal mRNA translation. There are three possible explanations: exosome binding and/or uptake stimulates target cells to initiate gene

transcription/silencing; transferred mRNA provides a trigger for master gene transcription; or miRNA allows for up-regulation of genes through silencing regulatory mRNA. We have not yet explored the first and second possibilities but searched for the impact of miRNA.

The Impact of Exosomal miRNA on LnStr and LuFb

A direct impact of exosomal miRNA on target cell mRNA was supported by the finding that 11 mRNAs with high signal strength in LnStr become downregulated by ASML[wt] and 18 mRNAs by ASML-CD44v[kd] exosomes (Figures 5A and 6A). Including mRNA with lower signal strength, 31 LnStr mRNAs were downregulated by ASML[wt] and/or ASML-CD44v[kd] exosomes. Similar to upregulated mRNA, mRNA down-regulation was mostly seen after co-culture with ASML[wt] and ASML-CD44v[kd] exosomes, although the degree of down-regulation differed. Down-regulation of MAL and cdh17 in LnStr co-cultured with ASML[wt] exosomes was confirmed by qRT-PCR, and at the protein level for MAL and GALs4 (ASML[wt] and ASML-CD44v[kd] exosomes), five of six genes were downregulated by ASML[wt] exosomes [periostin, aniline, cyclin B2, TNF receptor–associated factor 4 (TRAF4), and Cdc2a] and five of five genes were downregulated

by ASML-CD44v[kd] exosomes (claudin-6, neuropilin, ALDH3α1, IL1R1, and CA5b; Figure 6, B and C).

Curious, if exosomal miRNA might account for mRNA down-regulation, we searched (targetscan.org) for exosomal miRNA for which the target mRNA was downregulated in exosome-treated LnStr. We selected 20 mRNAs with high signal strength that were significantly downregulated after co-culture with ASML[wt] or ASML-CD44v[kd] exosomes. Arbitrarily taking these 20 mRNAs as 100% (inner circle), the relative reduction in co-cultures with ASML[wt] (middle circle) and ASML-CD44v[kd] exosomes (outer circle) was calculated (Figure 7A). Expectedly, several exosomal miRNAs could potentially account for down-regulation of these 20 mRNAs in LnStr; only the miRNAs potentially targeting the selected LnStr mRNAs are presented. The contribution of these miRNAs to the total recovery of exosomal miRNA is shown in the arrowed small circles (Figure 7B). As MAL, cdh17, and TRAF4 mRNA were strongly downregulated and, potentially targeting miR-494, miR-542-3p and miR-290 were enriched in ASML[wt] exosomes, we explored the effect of miRNA transfection on LnStr. miR-26b and miR-204, more abundant in ASML-CD44v[kd] exosomes and known to target Kruppel-like factor 4 (KLF4), whose expression was more strongly reduced in

Figure 7. Assignment of exosomal miRNA toward downregulated mRNA in LnStr. (A) Semiquantitative presentation of 20 abundant LnStr mRNAs that were strongly downregulated in exosome-treated LnStr. These 20 mRNAs have arbitrarily been taken as 100% (inner circle). The relative reduction by co-culture with ASML[wt] exosomes is shown in the middle circle and that by ASML-CD44v[kd] exosomes in the outer circle. (B) Exosomal miRNA potentially targeting these 20 downregulated LnStr mRNAs again were arbitrarily taken as 100%, their actual contribution to the total exosomal miRNA being indicated by the arrowed small circles. miRNA are assigned only for more than 50% reduced mRNA. Text box colors in A corresponds to text colors in B to facilitated coordination of potential effector miRNA in ASML[wt] (upper right) and ASML-CD44v[kd] exosomes (lower right) to the downregulated mRNA (abbreviations correspond to Figure 6).
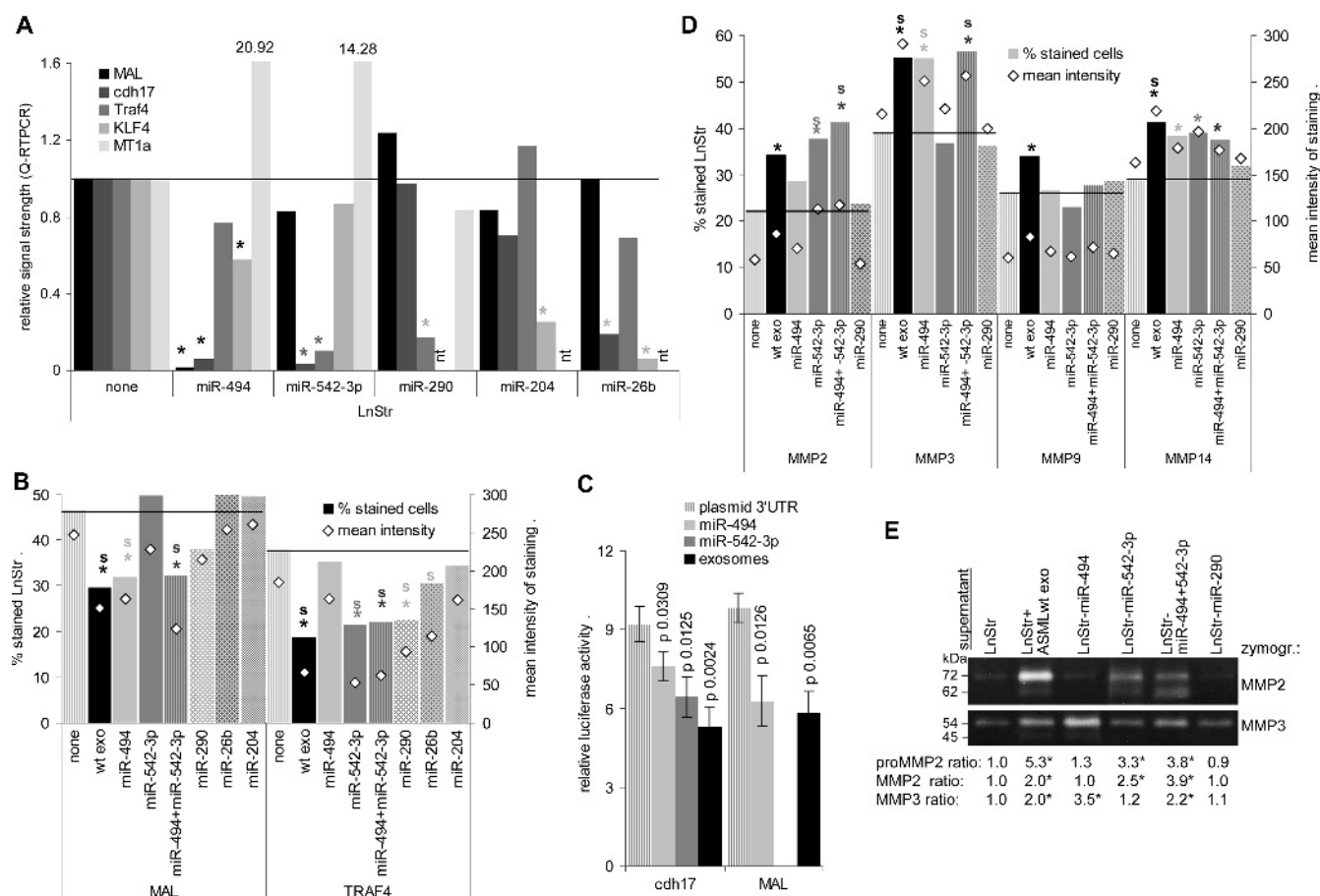
Figure 8. Functional activity of exosomal miRNA. (A and B) Impact of miR-494, miR-542-3p, miR-290, miR-204, and miR-26b transfection on MAL, cdh17, KLF4, and TRAF4 and, for comparison, MT1a expression in LnStr as revealed 48 hours after transfection or co-culture with exosomes by (A) qRT-PCR (mean of three replicate samples with SD < 0.25, indicating reliability according to the software program for ΔC_T) and (B) flow cytometry. (A) Significant differences in mRNA recovery between untreated and miRNA-transfected LnStr: *; (B) significant differences between untreated and miRNA-transfected LnStr in the mean percentage of stained cells (triplicates, two experiments): *; significant differences in the mean intensity of staining (triplicates, two experiments): **s**. (C) HEK293 cells were transfected with the dual-luciferase pmiRGlo vector containing the 3′UTR of MAL or cdh17 and were co-transfected with miR-494 or miR-542-3p (10 nM) or were co-cultured with ASML[wt] exosomes (20 μg). Firefly and, for normalization, Renilla luciferase activity was evaluated after 48 hours in a FLUOstar OPTIMA luminometer. The relative luciferase activity and *P* values for miR co-transfection or ASML[wt] exosome co-culture are shown. Significant differences are indicated. (D and E) Impact of cdh17 down-regulation in LnStr by miR-494 and/or miR-542-3p or, as control, miR-290 transfection on MMP2, MMP3, MMP9, and MMP14 expression as revealed by (D) flow cytometry and (E) representative example of zymography of LnStr culture supernatant, which confirmed MMP2 and MMP3 up-regulation. (D) Significant differences between untreated and miRNA-transfected LnStr in the mean percentage of stained cells (triplicates, two experiments): *; significant differences in the mean intensity of staining (triplicates): **s**. (E) The MMP ratio (mean of three experiments) compared to untreated LnStr is shown; significant differences: *. Transferred exosomal miRNA affects selective RNA expression in LnStr. As demonstrated for cdh17, exosomal miRNA repression of target mRNA can be accompanied by release of suppression for genes regulated by the primary miRNA target.

ASML-CD44v[kd]–treated LnStr, served as controls as well as MT1a, which is strongly upregulated in exosome-treated LnStr. qRT-PCR revealed down-regulation of MAL and cdh17 by miR-494, of cdh17 and TRAF4 by miR-542-3p, of TRAF4 by miR-290, and of KLF4 by miR-204 and miR-26b. The latter also affected cdh17, which is not a direct miR-26b target (Figure 8A). The findings were confirmed for MAL and TRAF4 protein expression in LnStr: miR-494 transfection downregulated MAL; miR-542-3p and miR-290 transfection downregulated TRAF4 expression, although with a lower efficacy than ASML[wt] exosomes; miR-26b and miR-204 transfection did not affect MAL; only miR-26b transfection weakly affected TRAF4 expression (Figure 8B). Furthermore, a 3′UTR MAL and cdh17 luciferase reporter assay confirmed that MAL and cdh17 are targeted by miR-494 and

cdh17 by miR-542-3p. Co-culture with ASML[wt] exosomes exerted a stronger effect than a single miRNA, indicating that additional exosomal miRNA may regulate cdh17 and MAL expression (Figure 8C). Thus, functional exosomal miRNA is transferred in LnStr and affects target gene expression.

MT1a mRNA up-regulation in LnStr upon co-culture with exosomes, but also by transfection with miR-494 and miR-542-3p, supported miRNA-mediated down-regulation of target mRNA to affect expression of genes regulated by the primary miRNA target. With the expression of several proteases being upregulated after co-culture with ASML exosomes despite low exosomal mRNA expression, we finally asked whether miRNA silencing of cdh17 might be accompanied by protease up-regulation, MMP2 and MMP9 up-regulation

being described to accompany cdh17 down-regulation [47]. Though expression of MMP9 was unaffected, MMP2 and MMP3 were strongly and MMP14 was weakly upregulated in miR-494, miR-542-3p, and miR-494 plus miR542-3p but not in control miR-290–transfected LnStr. miR-542-3p exerted a strong effect on MMP2 and miR-494 on MMP3 expression. MMP14 expression was equally affected by both miRNAs. Up-regulation of MMP2 and MMP3 in miRNA-transfected LnStr was confirmed by zymography (Figure 8, D and E).

Thus, tumor exosome miRNA strongly affects non-transformed target cells through silencing mRNA including mRNA up-regulation by release from repression by directly targeted mRNA.

Overview of Exosome-Modulated Gene Expression in Target Cells

Finally, we searched for functional activities of transcripts significantly upregulated by ASML[wt] exosomes in LnStr. For six genes, no or very preliminary data on functional activity were found (not settled). There has been no hint for up-regulation of oncogenes. Instead, increased protease activity, pronounced adhesion molecule and chemokine ligand expression, and up-regulation of cell cycle– and angiogenesis-promoting genes and of genes engaged in oxidative stress response all fit the demands of metastasizing tumor cells for settlement and growth (Figure W6).

Taken together, the transfer of exosomal miRNA has severe consequences on target cell gene expression, where miRNA-induced changes could facilitate metastasizing tumor cell settlement in pre-metastatic organs.

Discussion

Tumor cells can establish a niche for metastasizing cells preceding their arrival [3–5]. Tumor exosomes, carrying growth factors, cytokines/receptors, and matrix degrading enzymes and transferring tumor mRNA and miRNA [8,12,48], could well provide the essential trigger [6–8,10–12,15,16,49]. We showed [6] that poorly metastatic ASML-CD44v[kd] cells regain metastatic potential after conditioning rats with ASML[wt] or ASML-CD44v[kd] exosomes together with ASML[wt]-CM[−exo]. We here demonstrate that ASML exosomes are taken up *in vivo* and that exosomal miRNA strongly affects favorite targets shown for LnStr and LuFb. We particularly want to discuss two points: 1) Though exosomes are characterized by a protein profile that is rich in molecules located in internalization-prone membrane domains and molecules engaged in fission, scission, and vesicular transport [14,22,24,25], a single protein that is involved in gene transcription/posttranscriptional regulation, like CD44v, can have significant bearing on the composition of exosomal proteins, mRNA, and miRNA, even if not involved in directly guiding proteins or harboring mRNA/miRNA into MVB; 2) though we did not yet explore the impact of exosome binding– or uptake-induced signal transduction, our data support exosomal miRNA strongly affecting target cells.

Exosome Proteins, mRNA, and miRNA

Our findings confirm that recruitment of mRNA into MVB is a selective process such that the exosomal mRNA profile does not reflect that of the donor cell [18,22]. Only 1500 mRNAs were recovered in ASML exosomes compared to >8000 in ASML cells. This difference might be an overestimate as the mRNA isolation kit that was used mean-

while was demonstrated to unproportionally enrich for small RNA [46]. Nonetheless, the relative abundance of mRNA in exosomes and cells differed and there has been a significant number of mRNA that was enriched in exosomes compared to cells, strengthening the selective recruitment of mRNA into MVB. However, with few exceptions, the ratio of exosomal ASML[wt] *versus* ASML-CD44v[kd] mRNA did not differ significantly from that in cells. From there, we conclude that CD44v or associated molecules or molecules whose expression is regulated by CD44v may not be engaged in mRNA recruitment into MVB/exosomes. As already demonstrated [6,45], this also accounts for exosomal proteins. Protein expression differs between ASML[wt] and ASML-CD44v[kd] exosomes. However, these changes are also seen at the cellular level. However, CD44v/asssociated molecules clearly contribute to transcription of several genes recovered in exosomes, as the mRNA profile of ASML[wt] *versus* ASML-CD44v[kd] cells showed strong differences.

The cellular ASML[wt] and ASML-CD44v[kd] miRNA profiles also differ, suggesting engagement of CD44v/associated molecules in miRNA transcription or posttranscriptional regulation. Thus, the tumor suppressors let-7b, let-7d, let-7e, and miR-101 were increased in ASML-CD44[kd] exosomes and cells. It has been suggested that tumor cells get rid of let-7 through exosomes [50]. Alternatively, our findings point toward CD44v to be engaged in downregulating let-7 and miR-101. Irrespective of the underlying mechanism, the higher level of let-7 in ASML-CD44v[kd] exosomes is in line with the reduced metastatic capacity of these cells [43]. Notably, too, miR-34a, which suppresses tumor growth by CD44 down-regulation [51], was very low in ASML[wt] exosomes and cells but abundant in ASML-CD44v[kd] exosomes, which argues, in turn, for CD44v or associated molecules to be engaged in miR-34a silencing. Metastasis-promoting miR-494 and miR-21 and apoptosis-regulating miR-24-1 [52–54] are also abundant only in ASML[wt] exosomes. miRNA transcription and/or posttranscriptional regulation appear also to be affected by CD44v-associated c-Met [6], which supports miR-103 transcription [55] that is more than two-fold increased in ASML[wt] exosomes. CD44v-related changes are mostly reflected in the exosomal miRNA profile such that miRNA reduced in ASML-CD44v[kd] cells are also lower in ASML-CD44v[kd] than ASML[wt] exosomes. Irrespective of a possible additional involvement of CD44v in MVB recruitment, CD44v clearly is engaged in miRNA transcription/posttranscriptional regulation.

Taken together, proteins and mRNA of genes, whose expression is regulated by CD44v (http://www.ncbi.nlm.nih.gov/geo/query/acc.cgi?acc=GSE34739) [6,43,45], are recovered at a reduced level in ASML-CD44v[kd] exosomes. Yet, there is no evidence for CD44v contributing to protein or mRNA recruitment into MVB. Our data also indicate an engagement of CD44v in miRNA transcription/silencing/posttranscriptional regulation. Exosomal miRNA having a significant impact on target cells, the finding that a molecule not actively engaged in exosome assembly/transport can strongly affect the exosome composition requires detailed exploration that may provide key answers to metastasis-promoting CD44v activities.

Exosomal mRNA, miRNA, and Target Cell Fate

LnStr mRNA and protein recovery was altered by co-culture with ASML exosomes. Besides mRNA/miRNA, exosomal proteins can affect target cells as demonstrated for dendritic cell exosome–promoted T cell activation, which proceeds through exosome binding–initiated signal transduction and gene transcription [20]. Exosome binding–initiated signal transduction will be facilitated by exosomal ligands being located in internalization-prone membrane domains [33,56], which

are enriched in receptor tyrosine kinases, phosphatases, proteases, and, at the inner membrane, linker and signal transduction molecules [57]. Without question, target cell stimulation by tumor exosome binding and uptake requires to be evaluated. Nonetheless, we did not observe a measurable impact of exosomal proteins taken up by target cells [58] and high protein expression in ASML[wt] exosomes is hardly reflected by increased recovery in target cells. Therefore, we proceeded to ask for the impact of uptaken mRNA and miRNA. Though there are discrete differences in the mRNA and, more markedly, the miRNA profile of ASML[wt] and ASML-CD44v[kd] exosomes, it should be mentioned that we were mostly concerned about the impact of exosomal mRNA and miRNA in general and controlled at the functional level only ASML[wt] exosomes.

Similar to our findings on exosomal proteins, our data argue against transferred exosomal mRNA to account for increased target cell mRNA: 1) With few exceptions, mRNA levels are significantly higher in LnStr than exosomes; 2) mRNA levels become unproportionally upregulated, e.g., the MMP3 mRNA level in LnStr increased 13-fold upon exosome uptake, but the mRNA level in exosomes was about 10% that in LnStr, excluding the effect to be due to transferred exosomal mRNA; 3) mRNA levels in LnStr remained increased for 48 hours. RNA recovery in LnStr unlikely deriving from transferred exosomal mRNA points toward exosome-initiated transcription, which remains to be explored, or toward miRNA contributing to mRNA up-regulation by silencing repressive mRNA.

In LnStr co-cultured with ASML exosomes, several mRNA became strongly downregulated. Though it is not possible to differentiate between direct and indirect effects, as most miRNAs have multiple targets, there is evidence for a direct impact of exosomal miRNA. ASML[wt] and ASML-CD44v[kd] exosomes show distinct miRNA profiles and reduced mRNA levels in LnStr co-cultured with ASML[wt] versus ASML-CD44v[kd] exosomes overlap only partially. In addition, miRNA targeting mRNA selectively downregulated by ASML[wt] exosomes were more abundant in ASML[wt] than ASML-CD44v[kd] exosomes and the ASML-CD44v[kd] exosome miRNA that could potentially target the 18 mRNAs downregulated in LnStr accounts for more than 60% of the total miRNA.

We focused on abundant miR-494, potentially targeting MAL and cdh17, and miR-542-3p, targeting cdh17 and TRAF4. MAL can contribute to differentiation and apical sorting [59,60] and cdh17 to tumor growth/Wnt signaling [61]; TRAF4 exerts morphogenetic functions [62]. LnStr transfection with these miRNAs was accompanied by down-regulation of the predicted target(s), which also accounted for miR-204 and miR-26b transfection that downregulated KLF4, which can be opposingly affected by miRNA in normal versus malignant cells [63,64]. We confirmed by miRNA transfection and by luciferase reporter assay in co-culture with exosomes or transfection with miRNA that the transfer of exosomal miRNA can directly affect target cell mRNA.

Finally, significant up-regulation of mRNA in exosome-treated LnStr pointed toward mRNA up-regulation through miRNA silencing regulatory mRNA. Altered protease expression being a dominating feature in ASML-exosome–treated LnStr and in vivo in draining lymph nodes after ASML[wt]-CM application [6], and cdh17 down-regulation being known to promote MMP2 and MMP9 up-regulation [47], the finding that cdh17 down-regulation in miR-494 and miR-542-3p transfected LnStr was accompanied by MMP2, MMP3, and MMP14 up-regulation strengthens a direct impact of transferred exosomal miRNA on target cells.

Conclusion

Tumor exosomes being of central importance in premetastatic niche preparation [6,16], we characterized exosomes from a metastatic tumor line and evaluated their mode of action. CD44v contributing to the cross talk between tumor exosomes and host stroma, we additionally defined the impact of CD44v on the exosome composition.

As summarized in Figure W7, tumor exosomes contain a restricted mRNA and miRNA panel and there is evidence that CD44v contributes to shaping the exosomal protein, mRNA, and miRNA profiles by regulating gene and miRNA transcription/posttranscriptional regulation without a direct impact on recruitment into MVB/exosomes (Figure W7A). Exosomes reach premetastatic organs in vivo, bind, and are taken up by selected targets (Figure W7B). Exosome binding/uptake severely alters target cells. This can be due to exosome binding–initiated target modulation or target cell activation, which has not been explored in the present manuscript (Figure W7C), and to transferred exosomal miRNA, where we provide for the first time evidence that not only the direct miRNA target but also release from repression by the primary target significantly contributes to target cell reprogramming by tumor exosomes (Figure W7D). Finally, supporting the concept of a central role of tumor exosomes in metastasis, exosomal miRNA from a metastasizing tumor line, though not being oncogenic, preferentially regulates mRNA, which contributes to establishing a premetastatic niche (Figure W6).

Exosomes are discussed as a most potent gene delivery system. Our findings support this hypothesis and suggest that competing tumor exosomes could well be a promising therapeutic option by preventing establishing a premetastatic niche. Beyond this, tailored exosomes might allow to rescind tumor exosome–induced host cell modulation.

References

[1] Kraljevic Pavelic S, Sedic M, Bosnjak H, Spaventi S, and Pavelic K (2011). Metastasis: new perspectives on an old problem. *Mol Cancer* **10**, 22.

[2] Talmadge JE and Fidler IJ (2010). AACR centennial series: the biology of cancer metastasis: historical perspective. *Cancer Res* **70**, 5649–5669.

[3] Geiger TR and Peeper DS (2006). Metastasis mechanisms. *Biochim Biophys Acta* **1796**, 293–308.

[4] Kaplan RN, Rafii S, and Lyden D (2006). Preparing the "soil": the premetastatic niche. *Cancer Res* **66**, 11089–11093.

[5] McGovern M, Voutev R, Maciejowski J, Corsi AK, and Hubbard EJ (2009). A "latent niche" mechanism for tumor initiation. *Proc Natl Acad Sci USA* **106**, 11617–11622.

[6] Jung T, Castellana D, Klingbeil P, Cuesta Hernández I, Vitacolonna M, Orlicky DJ, Roffler SR, Brodt P, and Zöller M (2009). CD44v6 dependence of premetastatic niche preparation by exosomes. *Neoplasia* **11**, 1093–1105.

[7] Chairoungdua A, Smith DL, Pochard P, Hull M, and Caplan MJ (2010). Exosome release of β-catenin: a novel mechanism that antagonizes Wnt signaling. *J Cell Biol* **190**, 1079–1091.

[8] Hood JL, San Roman S, and Wickline SA (2011). Exosomes released by melanoma cells prepare sentinel lymph nodes for tumor metastasis. *Cancer Res* **71**, 3792–3801.

[9] Lee TH, D'Asti E, Magnus N, Al-Nedawi K, Meehan B, and Rak J (2011). Microvesicles as mediators of intercellular communication in cancer—the emerging science of cellular 'debris'. *Semin Immunopathol* **33**, 455–467.

[10] Lima LG, Chammas R, Monteiro RQ, Moreira ME, and Barcinski MA (2009). Tumor-derived microvesicles modulate the establishment of metastatic melanoma in a phosphatidylserine-dependent manner. *Cancer Lett* **283**, 168–175.

[11] McCready J, Sims JD, Chan D, and Jay DG (2010). Secretion of extracellular hsp90α via exosomes increases cancer cell motility: a role for plasminogen activation. *BMC Cancer* **10**, 294.

[12] Park JE, Tan HS, Datta A, Lai RC, Zhang H, Meng W, Lim SK, and Sze SK (2010). Hypoxic tumor cell modulates its microenvironment to enhance angiogenic and

metastatic potential by secretion of proteins and exosomes. *Mol Cell Proteomics* **9**, 1085–1099.

[13] Peinado H, Lavotshkin S, and Lyden D (2011). The secreted factors responsible for pre-metastatic niche formation: old sayings and new thoughts. *Semin Cancer Biol* **21**, 139–146.

[14] Rak J (2010). Microparticles in cancer. *Semin Thromb Hemost* **36**, 888–906.

[15] Ronquist KG, Ronquist G, Larsson A, and Carlsson L (2010). Proteomic analysis of prostate cancer metastasis-derived prostasomes. *Anticancer Res* **30**, 285–290.

[16] Peinado H, Alečković M, Lavotshkin S, Matei I, Costa-Silva B, Moreno-Bueno G, Hergueta-Redondo M, Williams C, García-Santos G, Ghajar C, et al. (2012). Melanoma exosomes educate bone marrow progenitor cells toward a pro-metastatic phenotype through MET. *Nat Med* **18**, 883–891.

[17] Mitchell PJ, Welton J, Staffurth J, Court J, Mason MD, Tabi Z, and Clayton A (2009). Can urinary exosomes act as treatment response markers in prostate cancer? *J Transl Med* **7**, 4.

[18] Wittmann J and Jäck HM (2010). Serum microRNAs as powerful cancer biomarkers. *Biochim Biophys Acta* **1806**, 200–207.

[19] Pap E, Pállinger E, Pásztói M, and Falus A (2009). Highlights of a new type of intercellular communication: microvesicle-based information transfer. *Inflamm Res* **58**, 1–8.

[20] Denzer K, Kleijmeer MJ, Heijnen HF, Stoorvogel W, and Geuze HJ (2000). Exosome: from internal vesicle of the multivesicular body to intercellular signaling device. *J Cell Sci* **113**(pt 19), 3365–3374.

[21] Lakkaraju A and Rodriguez-Boulan E (2008). Itinerant exosomes: emerging roles in cell and tissue polarity. *Trends Cell Biol* **18**, 199–209.

[22] Mathivanan S, Ji H, and Simpson RJ (2010). Exosomes: extracellular organelles important in intercellular communication. *J Proteomics* **73**, 1907–1920.

[23] van Niel G, Porto-Carreiro I, Simoes S, and Raposo G (2006). Exosomes: a common pathway for a specialized function. *J Biochem* **140**, 13–21.

[24] Raimondo F, Morosi L, Chinello C, Magni F, and Pitto M (2010). Advances in membranous vesicle and exosome proteomics improving biological understanding and biomarker discovery. *Proteomics* **11**, 709–720.

[25] Zöller M (2009). Tetraspanins: push and pull in suppressing and promoting metastasis. *Nat Rev Cancer* **9**, 40–55.

[26] Valadi H, Ekström K, Bossios A, Sjöstrand M, Lee JJ, and Lötvall JO (2007). Exosome-mediated transfer of mRNAs and microRNAs is a novel mechanism of genetic exchange between cells. *Nat Cell Biol* **9**, 654–659.

[27] Pant S, Hilton H, and Burczynski ME (2012). The multifaceted exosome: biogenesis, role in normal and aberrant cellular function, and frontiers for pharmacological and biomarker opportunities. *Biochem Pharmacol* **83**, 1484–1494.

[28] Gibbings DJ, Ciaudo C, Erhardt M, and Voinnet O (2009). Multivesicular bodies associate with components of miRNA effector complexes and modulate miRNA activity. *Nat Cell Biol* **11**, 1143–1149.

[29] Zomer A, Vendrig T, Hopmans ES, van Eijndhoven M, Middeldorp JM, and Pegtel DM (2010). Exosomes: fit to deliver small RNA. *Commun Integr Biol* **3**, 447–450.

[30] Atay S, Gercel-Taylor C, and Taylor DD (2011). Human trophoblast-derived exosomal fibronectin induces pro-inflammatory Il-1β production by macrophages. *Am J Reprod Immunol* **66**, 259–269.

[31] Escrevente C, Keller S, Altevogt P, and Costa J (2011). Interaction and uptake of exosomes by ovarian cancer cells. *BMC Cancer* **11**, 108.

[32] Rana S, Claas C, Kretz CC, Nazarenko I, and Zöller M (2011). Activation-induced internalization differs for the tetraspanins CD9 and Tspan8: impact on tumor cell motility. *Int J Biochem Cell Biol* **43**, 106–119.

[33] Rana S, Shijing Y, Stadel D, and Zöller M (2012). Toward tailored exosomes: the exosomal tetraspanin web contributes to target cell selection. *Int J Biochem Cell Biol* **44**, 1574–1584.

[34] Kosaka N, Iguchi H, Yoshioka Y, Takeshita F, Matsuki Y, and Ochiya T (2010). Secretory mechanisms and intercellular transfer of microRNAs in living cells. *J Biol Chem* **285**, 17442–17452.

[35] Lykke-Andersen S, Brodersen DE, and Jensen TH (2009). Origins and activities of the eukaryotic exosome. *J Cell Sci* **122**, 1487–1494.

[36] Hwang I and Ki D (2011). Receptor-mediated T cell absorption of antigen presenting cell-derived molecules. *Front Biosci* **16**, 411–421.

[37] Taylor DD and Gercel-Taylor C (2011). Exosomes/microvesicles: mediators of cancer-associated immunosuppressive microenvironments. *Semin Immunopathol* **33**, 441–454.

[38] Whiteside TL, Mandapathil M, Szczepanski M, and Szajnik M (2011). Mechanisms of tumor escape from the immune system: adenosine-producing Treg, exosomes and tumor-associated TLRs. *Bull Cancer* **98**, 25–31.

[39] Matzku S, Komitowski D, Mildenberger M, and Zöller M (1983). Characterization of BSp73, a spontaneous rat tumor and its *in vivo* selected variants showing different metastasizing capacities. *Invasion Metastasis* **3**, 109–123.

[40] Matzku S, Wenzel A, Liu S, and Zöller M (1989). Antigenic differences between metastatic and nonmetastatic BSp73 rat tumor variants characterized by monoclonal antibodies. *Cancer Res* **49**, 1294–1299.

[41] Günthert U, Hofmann M, Rudy W, Reber S, Zöller M, Haussmann I, Matzku S, Wenzel A, Ponta H, and Herrlich P (1991). A new variant of glycoprotein CD44 confers metastatic potential to rat carcinoma cells. *Cell* **65**, 13–24.

[42] Zöller M (2011). CD44: can a cancer-initiating cell profit from an abundantly expressed molecule? *Nat Rev Cancer* **11**, 254–267.

[43] Klingbeil P, Marhaba R, Jung T, Kirmse R, Ludwig T, and Zöller M (2009). CD44 variant isoforms promote metastasis formation by a tumor cell-matrix cross-talk that supports adhesion and apoptosis resistance. *Mol Cancer Res* **7**, 168–179.

[44] LeBedis C, Chen K, Fallavollita L, Boutros T, and Brodt P (2002). Peripheral lymph node stromal cells can promote growth and tumorigenicity of breast carcinoma cells through the release of IGF-I and EGF. *Int J Cancer* **100**, 2–8.

[45] Zech D, Rana S, Büchler MW, and Zöller M (2012). Tumor-exosomes and leukocyte activation: an ambivalent crosstalk. *Cell Commun Signal* **10**, 37.

[46] Eldh M, Lötvall J, Malmhäll C, and Ekström K (2012). Importance of RNA isolation methods for analysis of exosomal RNA: evaluation of different methods. *Mol Immunol* **50**, 278–286.

[47] Liu QS, Zhang J, Liu M, and Dong WG (2010). Lentiviral-mediated miRNA against liver-intestine cadherin suppresses tumor growth and invasiveness of human gastric cancer. *Cancer Sci* **101**, 1807–1812.

[48] Bussolati B, Grange C, and Camussi G (2011). Tumor exploits alternative strategies to achieve vascularization. *FASEB J* **25**, 2874–2882.

[49] Bobrie A, Krumeich S, Reyal F, Recchi C, Moita LF, Seabra MC, Ostrowski M, and Théry C (2012). Rab27a supports exosome-dependent and -independent mechanisms that modify the tumor microenvironment and can promote tumor progression. *Cancer Res* **72**, 4920–4930.

[50] Ohshima K, Inoue K, Fujiwara A, Hatakeyama K, Kanto K, Watanabe Y, Muramatsu K, Fukuda Y, Ogura S, Yamaguchi K, et al. (2010). Let-7 microRNA family is selectively secreted into the extracellular environment via exosomes in a metastatic gastric cancer cell line. *PLoS One* **5**, e13247.

[51] Liu C, Kelnar K, Liu B, Chen X, Calhoun-Davis T, Li H, Patrawala L, Yan H, Jeter C, Honorio S, et al. (2011). The microRNA miR-34a inhibits prostate cancer stem cells and metastasis by directly repressing CD44. *Nat Med* **17**, 211–215.

[52] Ali S, Almhanna K, Chen W, Philip PA, and Sarkar FH (2010). Differentially expressed miRNAs in the plasma may provide a molecular signature for aggressive pancreatic cancer. *Am J Transl Res* **3**, 28–47.

[53] Liu L, Jiang Y, Zhang H, Greenlee AR, and Han Z (2010). Overexpressed miR-494 down-regulates PTEN gene expression in cells transformed by anti-benzo(a)pyrene-trans-7,8-dihydrodiol-9,10-epoxide. *Life Sci* **86**, 192–198.

[54] Qin W, Shi Y, Zhao B, Yao C, Jin L, Ma J, and Jin Y (2010). miR-24 regulates apoptosis by targeting the open reading frame (ORF) region of FAF1 in cancer cells. *PLoS One* **5**, e9429.

[55] Garofalo M, Romano G, Di Leva G, Nuovo G, Jeon YJ, Ngankeu A, Sun J, Lovat F, Alder H, Condorelli G, et al. (2011). EGFR and MET receptor tyrosine kinase-altered microRNA expression induces tumorigenesis and gefitinib resistance in lung cancers. *Nat Med* **18**, 74–82.

[56] Rana S and Zöller M (2011). Exosome target cell selection and the importance of exosomal tetraspanins: a hypothesis. *Biochem Soc Trans* **39**, 559–562.

[57] Simons K and Gerl MJ (2010). Revitalizing membrane rafts: new tools and insights. *Nat Rev Mol Cell Biol* **11**, 688–699.

[58] Nazarenko I, Rana S, Baumann A, McAlear J, Hellwig A, Trendelenburg M, Lochnit G, Preissner KT, and Zöller M (2010). Cell surface tetraspanin Tspan8 contributes to molecular pathways of exosome-induced endothelial cell activation. *Cancer Res* **70**, 1668–1678.

[59] Brandt DT, Xu J, Steinbeisser H, and Grosse R (2009). Regulation of myocardin-related transcriptional coactivators through cofactor interactions in differentiation and cancer. *Cell Cycle* **8**, 2523–2527.

[60] Frank M (2000). MAL, a proteolipid in glycosphingolipid enriched domains: functional implications in myelin and beyond. *Prog Neurobiol* **60**, 531–544.

[61] Lee NP, Poon RT, Shek FH, Ng IO, and Luk JM (2010). Role of cadherin-17 in oncogenesis and potential therapeutic implications in hepatocellular carcinoma. *Biochim Biophys Acta* **1806**, 138–145.

[62] Mathew SJ, Haubert D, Krönke M, and Leptin M (2009). Looking beyond death: a morphogenetic role for the TNF signalling pathway. *J Cell Sci* **122**, 1939–1946.

[63] Lin CC, Liu LZ, Addison JB, Wonderlin WF, Ivanov AV, and Ruppert JM (2011). A KLF4-miRNA-206 autoregulatory feedback loop can promote or inhibit protein translation depending upon cell context. *Mol Cell Biol* **31**, 2513–2527.

[64] Papp B and Plath K (2011). Reprogramming to pluripotency: stepwise resetting of the epigenetic landscape. *Cell Res* **21**, 486–501.

Table W1. List of Antibodies.

Antibody	Supplier	Antibody	Supplier
α6β4	Clone B5.5 [1]	EpCAM	Clone D5.7 [1]
ADAM10	Santa Cruz Biotechnology (Heidelberg, Germany)	Fibulin	Santa Cruz Biotechnology
ADAM17	Santa Cruz Biotechnology	Fibronectin	BD (Heidelberg, Germany)
ADAMTS1	Santa Cruz Biotechnology	Follistatin	Santa Cruz Biotechnology
ADAMTS5	Santa Cruz Biotechnology	GADD45G	Santa Cruz Biotechnology
ADAMTS8	Santa Cruz Biotechnology	Gal.bind. 4	Santa Cruz Biotechnology
ALDH3a1	Santa Cruz Biotechnology	Hyaluronan	Rockland (Gilbertsville, PA)
Anillin	Santa Cruz Biotechnology	HGF	Santa Cruz Biotechnology
bFGF	Oncogene (Boston, MA)	HGDF	Santa Cruz Biotechnology
BTG2	Santa Cruz Biotechnology	IGF	Santa Cruz Biotechnology
CA5B	Santa Cruz Biotechnology	IL1Rl1	Santa Cruz Biotechnology
C4.4A	Clone C4.4 [1]	Laminin 1	Rockland
Caveolin	Santa Cruz Biotechnology	MAL	Santa Cruz Biotechnology
CD9	BD	MDR1	Santa Cruz Biotechnology
CD11a	BD	MMP2	Dianova (Hamburg, Germany)
CD11b	Clone Ox42 (EAACC)*	MMP3	Santa Cruz Biotechnology
CD11c	Clone Ox41 (EAACC)*	MMP9	Dianova
CD18	BD	MMP13	Dianova
CD24	BD	MMP14	Dianova
CD29	BD	Metallothio.	Santa Cruz Biotechnology
CD44s	Clone Ox50 (EAACC)*	Neuropilin	Santa Cruz Biotechnology
CD44v6	Clone A2.6 [1]	Osteopontin	Santa Cruz Biotechnology
CD49a	BD	Palladin	Santa Cruz Biotechnology
CD49b	BD	Pan cadherin	Santa Cruz Biotechnology
CD49c	BD	PDGF	BD
CD49d	BD	PDGFR	BD
CD49e	BD	Periostin	Santa Cruz Biotechnology
CD49f	Abcam (Cambridge, United Kingdom)	PG-Synth. 3	Santa Cruz Biotechnology
CD53	Clone Ox44 (EAACC)*	Phospholip.A2	Santa Cruz Biotechnology
CD54	Biozol (Eching, Germany)	Properdin	Santa Cruz Biotechnology
CD56	BD	SDF1	Abcam
CD61	Biozol	SLPI	Santa Cruz Biotechnology
CD62L	BD	SOD2	Santa Cruz Biotechnology
CD63	BD	Tenascin	LabVision (Fremont, CA)
CD81	Santa Cruz Biotechnology	TF	Santa Cruz Biotechnology
CD104	BD	TGFβ	Santa Cruz Biotechnology
CD106	Biozol	TRAF4	Santa Cruz Biotechnology
CD151	[2]	uPA	Calbiochem (Darmstadt, Germany)
Cdc2a	Santa Cruz Biotechnology	uPAR	Calbiochem
Claudin-4	Santa Cruz Biotechnology	VEGF	Biotrend (Köln, Germany)
Claudin-6	Santa Cruz Biotechnology	VEGFR1	Biotrend
Collagen I	Rockland	VEGFR2	Biotrend
Collagen II	LabVision	Vitronectin	Biotrend
Collagen IV	Rockland	vWF	Abcam
CXCR4	Santa Cruz Biotechnology	mIgG[†]	Dianova
CyclinB2	Santa Cruz Biotechnology	mIgM[†]	Dianova
D6.1A	Clone D6.1 [1]	Rabbit IgG[†]	Dianova
Endothelin	BD	Goat IgG[†]	Dianova
		Streptavidin[†]	Dianova

References:

[1] Matzku S, Wenzel A, Liu S, and Zöller M (1989). Antigenic differences between metastatic and non-metastatic rat tumor variants characterized by monoclonal antibodies. *Cancer Res* **49**, 1294–1299.
[2] Claas C, Wahl J, Orlicky D, Karaduman H, Schnölzer M, Kempf T, and Zöller M (2005). The tetraspanin D6.1A and its molecular partners on rat carcinoma cells. *Biochem J* **389**, 99–110.
*EAACC, European Association of Animal Cell Cultures, Porton Down, United Kingdom.
[†]Secondary antibodies and streptavidin were fluorescein isothiocyanate, phycoerythrin (PE), biotin, or HRP labeled.

Table W2. Primers.

Primers for qRT-PCR
GAPDH
Forward primer: cttctccatggtggtgaagac
Reverse primer: gaccccttcattgacctcaac
Cdh17
Forward primer: cctggtggtctctgtgaagg
Reverse primer: gtgattttgatggggtgagg
MAL
Forward primer: ttctccgtcttcgtcacctt
Reverse primer: gtctccccaccatgagtacc
KLF4
Forward primer: gcaagtcccctctctccatt
Reverse primer: ggtaaggtttctcgcctgtg
MMP3
Forward primer: ggctgaagatgacagggaag
Reverse primer: caatggcagaatccacactc
MT1a
Forward primer: accccaactgctcctgct
Reverse primer: acttgtccgaggcaccttt
ADAMTS1
Forward primer: gcccactgcttctactctgg
Reverse primer: gtgcgattgactcctccttc
TRAF4
Forward primer: gctgctggaggctgtcaa
Reverse primer: atctgtgctgggttcctg
4.5SRNA
Forward primer: aatgccccaaaaacagtcaa
Reverse primer: acctccagttgaaccagcac
C4.4A
Forward primer: attcacactcagcggttcct
Reverse primer: gtggtgggcttgatggtag
Stem loop primers
Universal reverse miRNA primer: 5′ gtgcagggtccgaggt 3′
Stem loop miR-300-5p:
Forward primer: 5′ gttggctctggtgcagggtccgaggtattcgcaccagagccaacacaaag 3′
Stem loop miR-296:
Forward primer: 5′ gttggctctggtgcagggtccgaggtattcgcaccagagccaacggagag 3′
Stem loop miR-300-5p:
Forward primer: 5′ gtttggttgaagagaggttatc 3′
Stem loop miR-296:
Forward primer: 5′ ttggagggttgggtggag 3′

Oligos and primers for the reporter assay
300-5p binding oligo
Sense: 5′ **aaac**tagcggccgctagtacaaaggataacctctcttcaa**t** 3′
Antisense: 5′ **ctaga**ttgaagagaggttatcctttgtactagcggccgcta**gttt** 3′
Cdh17
3′UTR cdh17 fw Pme1: gtttaaactccctttctgtttccacctg
3′UTR cdh17 rev Xba1: tctagacaccacgtacatgctttcgt
MAL
3′UTR MAL fw Pme1: gtttaaacgacagcagattgggagct
3′UTR MAL rev Xba1: tctagatgttgggtgaatttcagtg

Sequences of the 3′UTR with binding sites and SVR score
3′UTR MAL
gacagcagattgggagctgaaacccagagcaattaactggtcagcctgtcttccccattaacttcctggaacagactgaatggtggagaaaagaaaa
caagccaaaagaaaacaaaacagacacaaaaacaaaaggaaaccatgttcgagtctcttgggtgttacgtttaccttctgttagggtttagggcttg
ctgaatttaacttccagccaaaggaggaaagagttgtcttggcgggccctttctgcccttgaccaggacagtgggtgggagcttggaaccttgatc
tgaagaaatgacaatttccccttgacccttggagcaggtcctaacaattgcctttcggaattttccacaagctctttgcaccactcatcccctggcata
tcttagattttgtggatagtctaggtgtcacaggcactgaaattcacccaaca
gacagcagattgggagc: target site miR-494 (mirSVR score: –0.9472)
3′UTR Cdh17
tccctttctgtttccacctgcgcccctgatctcagcattacattaaatttaaaatgtgtcacacaaaagaacaaagtgaagtccttggggggggtgtt
gctaagtggacagccttattctttagcacaaacaacagcttctctgtgttgtcatctttaatagaggtcctccagcttggctatggtgtagaccctggg
gaggtatcaaatacaactgccgtgtttcaagaaagacctacttcatgaggcacaggaactgacgagctgtctgggtttactcactactccgtgctta
catacatgctgtacatgttttatttgtatattgaagttttgttatatatttatcatgtggaggaaagacgaaagcatgtacgtggtg
attaaatttaaaatgtgtcaca: target site miR-542-3P (mirSVR score: –0.1085)
atacatgctgtacatgtttta: target site miR 494 (mirSVR score: –0.1085)

Table W3. mRNA Recovery in ASML^{wt} and ASML-CD44v^{kd} Exosomes (Signal Strength 10,000).

mRNA	Mean Signal Strength*	
	ASML^{wt} Exosomes	ASML-CD44v^{kd} Exosomes
Acidic ribosomal phosphoprotein P0 (Arbp)	36,537	34,209
Pred. similar to LRRG00135	28,102	17,532
Pred. similar to Ab2-143	26,757	13,956
Pred. similar to 60S ribosomal protein L37a	25,511	27,156
Pred. similar to LRRG00135	25,318	15,450
Pred. similar to testin (LOC503278)	24,223	12,457[†]
Pred. similar to RIKEN cDNA 2410116I05	23,944	21,405
Ribosomal protein S15a (Rps15a)	22,854	25,011
Pred. ribosomal protein L27a (Rpl27a)	21,294	25,079
Pred. ribosomal protein L37a (Rpl37a)	20,655	26,661
Pred. similar to 60S ribosomal protein L7a	18,819	24,078
Ribosomal protein S14 (Rps14)	18,335	22,643
Eukaryotic translation elongation factor 1 alpha 1	17,840	20,172
Pred. similar to ORF4	17,709	8,172[†]
Pred. similar to 60S ribosomal protein L23a	17,248	22,830
Pred. similar to ribosomal protein L19	16,799	21,770
Pred. similar to ORF4 (LOC361942)	16,503	7,596[†]
Ribosomal protein S18 (Rps18)	16,501	16,624
Pred. similar to testis-derived transcript	16,125	25,111
Pred. ribosomal protein L10 (Rpl10)	16,056	14,972
Ribosomal protein L41 (Rpl41)	15,816	15,564
Pred. S100 calcium-binding protein A11 (S100a11)	15,812	20,179
Pred. similar to 40S ribosomal protein S3	15,623	14,168
Ribosomal protein S4, X-linked (Rps4x)	15,608	22,525
Pred. ribosomal protein s25 (Rps25)	15,597	15,107
Pred. similar to Ac1262	15,361	6,541[†]
Ribosomal protein L9 (Rpl9)	15,328	15,018
Tumor protein, translationally controlled 1 (Tpt1)	14,796	15,898
Pred. similar to 60S ribosomal protein L7a	14,785	18,844
Ferritin, heavy polypeptide 1 (Fth1)	14,268	13,168
Ribosomal protein L29 (Rpl29)	14,249	19,063
Eukaryotic translation elongation factor 1 alpha 1	14,047	15,670
Pred. ribosomal protein S5 (Rps5)	13,772	12,954
Ribosomal protein L3 (Rpl3)	13,516	17,927
Laminin receptor 1 (ribosomal protein SA) (Lamr1)	13,281	16,180
Ribosomal protein S3 (Rps3)	13,274	13,387
Ribosomal protein L32 (Rpl32)	13,223	14,601
Ribosomal protein L6 (Rpl6)	13,023	13,800
Pred. similar to glyceraldehyde-3-phosphate dehydrogenase	12,883	20,653
Ribosomal protein S10 (Rps10)	12,629	15,551
Ribosomal protein S29 (Rps29)	12,375	14,993
Ribosomal protein S20 (Rps20)	12,191	16,162
Pred. Similar to 60S ribosomal protein L9	12,045	11,228
Pred. similar to 60S ribosomal protein L6 (neoplasm-related protein C140)	12,002	11,535
Pred. similar to ribosomal protein S7	11,952	16,878
Pred. similar to 40S ribosomal protein S20	11,767	13,423
Pred. similar to ribosomal protein S23	11,758	14,377
Pred. similar to ribosomal protein S26	11,619	11,565
Ribosomal protein L17 (Rpl17)	11,387	14,337
Pred. similar to ribosomal protein L15	11,382	10,145
Ubiquitin A-52 residue ribosomal protein fusion product 1	11,277	10,050
Pred. similar to Finkel-Biskis-Reilly murine sarcoma virus (FBR-MuSV) ubiquitously expressed (fox derived)	11,094	13,392
Ribosomal protein S8 (Rps8)	11,085	17,872
Ribosomal protein L22 (Rpl22)	11,074	15,648
Pred. similar to ribosomal protein L31	11,007	12,825
Pred. similar to 60S ribosomal protein L32	10,602	12,524
Ribosomal protein, large, P1 (Rplp1)	10,529	9,656
Ribosomal protein S26 (Rps26)	10,390	11,011
Peptidylprolyl isomerase A (Ppia)	10,363	18,435
Ribosomal protein L27 (Rpl27)	10,242	14,789
Pred. Finkel-Biskis-Reilly murine sarcoma virus ubiquitously expressed (Fau)	10,237	13,329
Pred. similar to 60S ribosomal protein L17 (L23) (amino acid starvation–induced protein) (ASI)	10,203	12,418
Pred. similar to tubulin alpha-2 chain (alpha-tubulin 2)	8,769	20,050[†]
Actin, beta (Actb)	7,779	14,422
Ribosomal protein L19 (Rpl19)	9,245	12,973
Pred. similar to L-lactate dehydrogenase A chain	8,749	12,938
Pred. capping protein (actin filament) muscle Z-line, α2	9,542	12,599
Pred. similar to ribosomal protein S12	9,387	12,278
Pred. similar to 60S acidic ribosomal protein P2	8,699	12,266
Calmodulin 2 (Calm2)	7,108	12,054
Pred. similar to 60S ribosomal protein L7a	9,513	12,043
Ribosomal protein L21 (Rpl21)	8,710	11,910

Table W3. (continued)

mRNA	Mean Signal Strength*	
	ASML^wt Exosomes	ASML-CD44v^kd Exosomes
Pred. similar to ribosomal protein L21	9,121	11,850
Pred. triosephosphate isomerase 1 (Tpi1)	5,867	11,739[†]
PAI-1 mRNA-binding protein (Pairbp1)	5,297	11,647[†]
Pred. glutathione S-transferase, pi 1 (Gstp1)	7,189	11,480
Pred. similar to glyceraldehyde-3-phosphate dehydrogenase	9,042	11,083
Ribosomal protein S6 (Rps6)	8,109	10,953
Pred. similar to ribosomal protein S19	7,851	10,950
Large subunit ribosomal protein L36a (Rpl36a)	8,625	10,804
Pred. actin, gamma, cytoplasmic (Actg)	8,184	10,751
Similar to 60S ribosomal protein L21	7,251	10,610
Pred. similar to 40S ribosomal protein S3a (V-fos transformation effector protein)	6,252	10,107
Ornithine decarboxylase antizyme 1 (Oaz1)	6,971	10,027

*Mean signal strength was calculated from duplicates, respectively, triplicates, of two independently performed arrays after normalization (Chipster analysis and Agilent annotation). Only exosomal mRNA with a signal strength of >10,000 is shown.
[†]Signal strength with a more than two-fold change between ASML^wt and ASML-CD44v^kd exosomes.

Table W4. mRNA Expression in ASML^wt and ASML-CD44v^kd Cells (Signal Strength 50,000).

mRNA	Mean Signal Strength*	
	ASML^wt Cells	ASML-CD44v^kd Cells
Hypothetical protein LOC310926	299,044	309,590
Actin, gamma 1 (Actg1)	296,979	221,969
Stefin A2 (Stfa2)	294,927	329,519
Ferritin, light polypeptide (Ftl)	246,290	277,091
Heat shock protein 8 (Hspa8)	246,290	143,431
Finkel-Biskis-Reilly murine sarcoma virus (FBR-MuSV)	223,513	182,812
Similar to TRAF-binding protein	217,401	260,333
Testis-derived transcript (Tes)	214,408	143,431
Ferritin light chain 1-like	209,996	217,401
Similar to Ac1147	205,674	221,969
Carcinoembryonic antigen-related cell adhesion molecule 9 (Ceacam9)	202,842	249,728
Similar to glyceraldehyde-3-phosphate dehydrogenase	193,235	180,295
Similar to Rpl7a protein	193,235	179,050
Eukaryotic translation elongation factor 1 gamma (Eef1g)	168,221	91,406
Enolase 1 alpha	165,905	200,050
Ferritin heavy polypeptide 1 (Fth1)	162,491	121,450
Ubiquitin A-52 residue ribosomal protein fusion product 1 (Uba52)	162,491	133,826
Phosphoglycerate mutase 1 (brain) (Pgam1)	159,147	90,775
Similar to sex-determination protein homolog Fem1a	158,048	155,872
Similar to DKFZP434B168 protein	155,872	134,757
Peptidylprolyl isomerase A (cyclophilin A) (Ppia)	151,609	182,812
Coiled-coil-helix-coiled-coil-helix domain containing 2 (Chchd2)	150,562	111,757
Eukaryotic translation elongation factor 1 alpha 1 (Eef1a1)	147,464	151,609
Annexin A2 (Anxa2)	145,433	133,826
Similar to cleavage and polyadenylation factor 73 kDa (CPSF73kDa)	142,441	136,638
Phosphoglycerate kinase 1 (Pgk1)	136,638	100,721
Lactate dehydrogenase A (Ldha)	135,694	95,950
Similar to glyceraldehyde-3-phosphate dehydrogenase	135,694	118,129
Annexin A1 (Anxa1)	129,267	101,421
Heat shock protein HSP 90-beta	125,733	85,878
Transketolase (Tkt)	125,733	107,204
Capping protein (actin filament) muscle Z-line, alpha 2 (Capza2)	122,295	73,732
Eukaryotic translation initiation factor 2B, subunit 2 beta (Eif2b2)	120,611	105,728
Similar to elongation factor 1-alpha 1 (EF-1-alpha-1)	117,313	107,950
Heat shock cognate 71 kDa protein	115,698	66,451
Cathepsin D (Ctsd)	114,105	153,726
Similar to peptidylprolyl isomerase A (cyclophilin A)	110,985	137,588
Actin, beta (Actb)	106,464	48,645[†]
Ubiquitin C (Ubc)	106,464	146,445
Tumor protein translationally controlled 1 (Tpt1)	104,273	153,726
Eukaryotic translation elongation factor 1 beta 2 (Eef1b2)	100,721	102,127
Ubiquitin B (Ubb)	97,290	95,950
Keratin 18 (Krt18)	95,950	19,216[†]
Hypothetical gene supported by AF152002 (LOC290595)	94,629	56,267
Tubulin beta 4B class IVb (Tubb4b)	93,976	72,717
Transmembrane emp24-like trafficking protein 10 (Tmed10)	91,406	131,984
Interferon gamma–induced GTPase (Igtp)	90,775	113,317

Table W4. (*continued*)

mRNA	Mean Signal Strength*	
	ASML^wt Cells	ASML-CD44v^kd Cells
Similar to elongation factor 1-gamma (EF-1-gamma)	90,775	40,342[†]
Glutathione *S*-transferase pi 1 (Gstp1)	86,475	53,232
Heat shock protein 1 (chaperonin 10) (Hspe1)	86,475	50,360
Glutathione peroxidase 2 (Gpx2)	85,285	13,401[†]
Nucleophosmin (nucleolar phosphoprotein B23, Numatrin) (Npm1)	84,111	92,682
RAN member RAS oncogene family (Ran)	84,111	69,273
Progressive external ophthalmoplegia 1 (Peo1)	81,811	182,812[†]
Hypothetical protein LOC687872	79,024	71,220
Eukaryotic translation elongation factor 1 delta (Eef1d)	77,398	60,725
Poly(A)-binding protein, cytoplasmic 1 (Pabpc1)	77,398	115,698
Eukaryotic translation elongation factor 2 (Eef2)	76,863	38,166[†]
Guanine nucleotide binding protein beta polypeptide 2 like 1 (Gnb2l1)	76,332	39,512
Cytochrome *c* oxidase subunit VIa polypeptide 1 (Cox6a1)	75,281	139,509
NADH-ubiquinone oxidoreductase chain 1	74,761	209,996[†]
Cytochrome *c* oxidase subunit VIIa polypeptide 2 like (Cox7a2l)	73,732	64,634
Mitogen-activated protein kinase 3 (MAPK3)	73,732	80,684
Galactoside-binding soluble 3 (Lgals3)	73,223	80,684
Cytochrome *b*	72,717	181,549[†]
Non-metastatic cells 2 protein (NM23B) (Nme2)	72,717	65,083
Myosin light polypeptide 6 smooth muscle and non-muscle-like (Myl6l)	72,214	105,728
RT1 class Ia, locus A1 (RT1-A1)	71,716	90,775
Cell division cycle 37 homolog (Cdc37)	69,755	46,988
Glyceraldehyde-3-phosphate dehydrogenase (GAPDH)	69,755	52,864
CD24	69,273	28,725
Complement component 1q subcomponent binding protein (C1qbp)	69,273	67,847
Hematological and neurological expressed 1 (Hn1)	69,273	22,073[†]
ATP synthase, H+ transporting, mitochondrial Fo complex C2 (Atp5g2)	68,794	53,602
Phosphoglycerate dehydrogenase (Phgdh)	68,319	72,214
Proteasome subunit beta type 4 (Psmb4)	68,319	39,512
Heat shock protein 90 alpha class B member 1 (Hsp90ab1)	67,378	44,762
Ornithine decarboxylase antizyme 1 (Oaz1)	67,378	62,432
Similar to glyceraldehyde-3-phosphate dehydrogenase	67,378	52,864
ATP synthase, H+ transporting, mitochondrial Fo complex d (Atp5h)	66,913	72,214
Thymosin beta 4. X-linked (Tmsb4x)	66,913	55,109
High-mobility group nucleosome binding domain 1 (Hmgn1)	65,992	85,878
Phosphatidylethanolamine-binding protein 1 (Pebp1)	65,992	76,332
Histidine triad nucleotide-binding protein 1 (Hint1)	65,536	74,761
Eukaryotic translation initiation factor 3, subunit I (Eif3i)	65,083	59,889
ATP synthase subunit d	64,634	65,992
Heat shock protein 1 (chaperonin) (Hspd1)	64,187	50,360
Similar to RIKEN cDNA 3100001N19 (LOC306079)	63,304	54,728
H6 family homeobox 1 (Hmx1)	62,866	59,064
GNAS complex locus (Gnas), transcript variant 3	62,432	120,611
Ly6/Plaur domain containing 3 (Lypd3)	62,432	45,703
ATP synthase, H+ transporting, mitochondrial Fo complex E (Atp5i)	61,573	64,187
Similar to glyceraldehyde-3-phosphate dehydrogenase (LOC305194)	61,573	47,315
Prothymosin alpha (Ptma)	59,475	59,889
Family with sequence similarity 49, member B (Fam49b)	58,251	49,667
ADP-ribosylation factor 5 (Arf5)	57,449	32,317
GTPase IMAP family member 9 (Gimap9)	57,449	75,805
Enolase 1alpha (Eno1) transcript variant 2	57,052	70,728
Cysteine-rich protein 2 (Crip2)	56,658	42,055
ATP synthase, H+ transporting, F1 complex α1 cardiac muscle (Atp5a1)	55,878	67,378
Reactive oxygen species modulator 1 (Romo1)	55,878	32,768
Proteasome 26S subunit ATPase 5 (Psmc5)	55,492	26,801[†]
TIMP metallopeptidase inhibitor 2 (Timp2)	55,109	214,408[†]
Cytochrome *c* oxidase subunit 1	53,975	190,575[†]
Eukaryotic translation initiation factor 4H (Eif4h)	51,776	21,469[†]
T-box 21 (Tbx21)	51,776	48,983
Destrin (Dstn)	51,419	36,358
Similar to keratin complex 1 acidic gene 18	51,419	7,913[†]
Mesothelin (Msln)	51,063	58,251
Tubulin, alpha 1B (Tuba1b)	50,012	63,744
ATP synthase subunit a	38,699	208,545[†]
Cytochrome *c* oxidase subunit 3	42,348	167,059[†]
S100 calcium-binding protein A6 (S100a6)	40,623	165,905[†]
Caveolin 1 (Cav1)	43,238	155,872[†]
Cytochrome *c* oxidase subunit 2	39,787	146,445[†]
NADH-ubiquinone oxidoreductase chain 4	34,397	128,375[†]
Kelch domain containing 2 (Klhdc2)	38,431	100,721[†]
ATP synthase F1 complex epsilon (Atp5e)	40,623	94,629[†]
Growth arrest specific 5 (Gas5)	42,055	93,976[†]

mRNA	Mean Signal Strength*	
	ASML^wt Cells	ASML-CD44v^kd Cells
S100 calcium-binding protein A4 (S100a4)	5,405	90,148[†]
Serum deprivation response (Sdpr)	24,154	85,285[†]
Dynein heavy-10 (Dnah10)	49,667	78,478
Rap GEF 6 (Rapgef6)	48,983	77,936
NADH-ubiquinone oxidoreductase chain 2	7,750	72,717[†]
SMT3 suppressor of mif two 3 homolog 2 (Sumo2)	49,667	70,728
Caveolin 2 (Cav2)	23,170	68,794[†]
Thioredoxin 1 (Txn1)	44,453	66,913
Myosin light chain 6 (Myl6)	46,341	65,992
Translationally controlled tumor protein (TCTP)	43,538	65,536
Hepatocyte malignant transforming factor	38,431	65,083
Ubiquinol-cytochrome *c* reductase complex isoform b	43,841	62,866
Eukaryotic translation initiation factor 4E binding protein 1 (Eif4ebp1)	34,397	62,432
Cathepsin B (Ctsb)	36,611	60,725
Stearoyl-CoA desaturase delta (Scd)	23,494	59,064[†]
Parkinson protein 7 (Park7)	37,902	57,849
Glutathione peroxidase 4 (Gpx4)	46,021	57,449
Acidic (leucine-rich) nuclear phosphoprotein 32B (Anp32b)	27,175	57,449
Clathrin light chain A (Clta)	29,944	56,267
Suppressor of initiator codon mutations	33,225	54,728
Aminolevulinate dehydratase (Alad)	38,699	54,350
Protein tyrosine phosphatase F (Ptprf)	15,076	53,602[†]
H1 histone family member 0 (H1f0)	5,043	53,232[†]
Histone cluster 1 H2ak (Hist1h2ak)	44,762	52,864
2-5 oligoadenylate synthetase 1B (Oas1b)	35,120	52,499
Eukaryotic translation initiation factor 3K (Eif3k)	48,645	50,711
Cyclin-dependent kinase inhibitor 2A (Cdkn2a)	27,746	50,711
Programmed cell death 5 (Pdcd5)	28,329	50,360

*Mean signal strength was calculated from duplicates, respectively, triplicates, after normalization (Chipster analysis and Agilent annotation) of two independently performed microarray analyses. Only cellular mRNA with a signal strength of >50,000 is shown.
[†]Signal strength with a more than two-fold change between ASML^wt and ASML-CD44v^kd cells.

Table W5. Distinctly Recovered mRNA in ASML^wt and ASML-CD44v^kd Exosomes *versus* Cells.

mRNA	Mean Signal Strength*		ASML^wt Exosomes *versus* Cells	Mean Signal Strength*		ASML-CD44v^kd Exosomes *versus* Cells
	ASML^wt			ASML-CD44v^kd		
	Exosomes	Cells		Exosomes	Cells	
Translationally controlled tumor protein 1 (Tpt1)	21,555	104,273	0.21	20,863	153,726	0.14
Ferritin 1 (Fth1)	21,061	169	124.70	18,061	131	138.20
Laminin receptor 1 (Lamr1)	19,878	nd[†]	∞	20,967	nd	∞
Keratin complex 1-19 (Krt1-19)	14,348	73	197.89	13,274	79	168.47
Actin, beta (Actb)	12,963	106,464	0.12	18,280	48,645	0.38
Calmodulin 2 (Calm2)	12,033	51,776	0.23	15,726	60,725	0.26
Ornithine decarboxylase antizyme 1 (Oaz1)	11,924	90	132.67	13,427	80	166.90
Metallothionein (MT1a)	9,659	596	16.20	5,546	526	10.54
Peroxiredoxin 1 (Prdx1)	9,436	77	122.27	12,336	104	118.65
Non-metastatic cells 2 (Nme2)	9,417	nd	∞	9,113	nd	∞
Phosphoglycerate kinase 1 (Pgk1)	9,391	89	105.21	12,013	131	91.92
Annexin A2 (Anxa2)	9,196	145,433	0.06	8,734	133,826	0.07
Synaptic vesicle glycoprotein 2b (Sv2b)	9,153	nd	∞	3,304	nd	∞
Annexin A1 (Anxa1)	9,072	129,267	0.07	9,408	101,421	0.09
Villin 2 (Vil2)	9,071	nd	∞	7,751	nd	∞
Diazepam binding inhibitor (Dbi)	8,840	80	109.88	10,165	78	130.81
Macrophage migration inhibitory factor (Mif)	8,578	135	63.40	9,533	85	112.10
Galactose binding lectin, soluble 3 (Lgals3)	8,566	72	119.79	6,559	68	96.29
Peroxiredoxin 2 (Prdx2)	8,476	370	22.93	10,633	187	56.74
Cell division cycle 37 homolog (Cdc37)	8,377	405	20.71	11,208	269	41.71
S100 calcium-binding protein A6 (S100a6)	8,297	1,287	6.44	7,497	357	21.00
Brain protein I3 (Bri3)	8,064	21,028	0.38	10,520	15,936	0.66
Cofilin 1 (Cfl1)	8,043	46,988	0.17	12,817	25,709	0.50
Basic keratin complex 2-8 (Krt2-8)	8,015	nd	∞	7,486	nd	∞
Phosphatidylethanolamine-binding protein (Pbp)	7,653	843	9.07	8,791	867	10.14
Proteasome subunit beta 1 (Psmb1)	7,626	80	95.46	8,227	68	121.61
Aldose reductase 1-B4 (Akr1b4)	7,411	4,096	1.81	8,827	2,937	3.01

mRNA	Mean Signal Strength*		ASML[wt] Exosomes versus Cells	Mean Signal Strength*		ASML-CD44v[kd] Exosomes versus Cells
	ASML[wt]			ASML-CD44v[kd]		
	Exosomes	Cells		Exosomes	Cells	
Profilin 1 (Pfn1)	6,662	187	35.55	5,998	67	89.27
Heat shock protein 8 (Hspa8)	6,577	6,165	1.06	4,584	3,236	1.41
Cell division cycle 42 (Cdc42)	6,492	519	12.51	10,242	298	34.35
Glutathione peroxidase 2 (Gpx2)	6,434	1,226	5.25	4,124	1,209	3.41
Cytochrome *c*, somatic (Cycs)	6,401	343	18.69	8,157	910	8.96
Protein phosphatase 1-14B (Ppp1r14b)	6,280	34,397	0.18	4,807	22,227	0.22
Adaptor-related protein complex 2-sigma 1 (Ap2s1)	6,237	21,619	0.29	7,003	12,944	0.54
Transmembrane trafficking protein 21 (Tmp21)	6,161	nd	∞	5,505	nd	∞
Proliferating cell nuclear antigen (Pcna)	5,845	21,469	0.27	7,698	11,426	0.67
Tyrosine 3-monooxygenase/tryptophan 5-monooxygenase activation protein, zeta (Ywhaz)	5,843	4,012	1.46	7,178	5,293	1.36
Proteasome beta-4 (Psmb4)	5,697	5,113	1.11	6,876	1,053	6.53
Superoxide dismutase 1 (Sod1)	5,639	49,324	0.11	6,120	33,225	0.18
ATPase, H+ transporting, V0-C (Atp6v0c)	5,550	13,777	0.40	5,220	10,441	0.50
Proteolipid protein 2 (Plp2)	5,549	3,692	1.50	4,413	4,939	0.89
Non-metastatic cells 1 (Nme1)	5,487	20,453	0.27	5,242	16,845	0.31
C-terminal binding protein 1 (Ctbp1)	5,416	24,492	0.22	8,964	11,191	0.80
ARP2 actin-related 2 (Actr2)	5,387	5,914	0.91	7,636	5,480	1.39
Cytochrome *c* oxidase VIIb (Cox7b)	5,263	74	71.59	5,238	69	75.83
Integrin beta 4 binding protein (Itgb4bp)	5,252	8,719	0.60	4,039	27,939	0.14
Proteasome beta 2 (Psmb2)	5,169	176	29.36	5,941	74	80.81
Radixin (Rdx)	5,165	17,929	0.29	4,787	187	25.54
Cyclin D1 (Ccnd1)	5,160	4,576	1.13	8,670	1,783	4.86
Peptidylprolyl isomerase B (Ppib)	5,083	68	75.14	3,001	72	41.68
S-phase kinase-associated 1A (Skp1a)	4,916	10,369	0.47	5,992	5,914	1.01
Tubulin beta 2 (Tubb2)	4,851	609	7.97	6,840	1,160	5.90
SMT3 suppressor of mif two 3-1 (Sumo1)	4,843	7,913	0.61	7,168	8,192	0.88
Glutathione peroxidase 4 (Gpx4)	4,840	93	52.01	4,487	75	60.19
Chromobox homolog 3 (Cbx3)	4,839	1,113	4.35	5,945	798	7.45
Poly(A)-binding protein 1 (Pabpc1)	4,788	186	25.73	3,177	239	13.30
Dynein light chain 2A (Dncl2a)	4,747	2,320	2.05	3,733	1,003	3.72
Aldo-keto reductase 1-A1 (Akr1a1)	4,656	9,345	0.50	7,095	12,161	0.58
Tyrosine 3/tryptophan 5-monooxygenase ε (Ywhae)	4,646	31,433	0.15	9,089	33,689	0.27
MAP kinase kinase 2 (Map2k2)	4,573	30,362	0.15	4,357	26,801	0.16
S100 calcium-binding protein A4 (S100a4)	4,495	92	48.98	4,424	1,261	3.51
Dynein light chain 1 (Dnclc1)	4,444	333	13.34	3,237	508	6.37
ATX1-1 (Atox1)	4,389	13,308	0.33	3,323	6,383	0.52
Beta-2 microglobulin (B2m)	4,380	26,987	0.16	3,997	22,694	0.18
Aldolase A (Aldoa)	4,313	19,619	0.22	2,549	8,841	0.29
Lactate dehydrogenase A (Ldha)	4,278	333	12.84	3,623	498	7.28
RAN, member RAS oncogene family (Ran)	4,266	72	59.66	4,704	167	28.24
Hepatoma-derived growth factor (Hdgf)	4,232	48,309	0.09	5,068	35,364	0.14
Catenin alpha 1 (Catna1)	4,168	3,169	1.32	7,307	3,083	2.37
Complement component 1q (C1qbp)	4,158	516	8.07	4,389	2,759	1.59
Fertility protein SP22 (Park7)	4,146	nd	∞	5,720	nd	∞
Thioredoxin 1 (Txn1)	4,141	44,453	0.09	3,567	66,913	0.05
Chaperonin subunit 4 (Cct4)	4,101	127	32.26	4,233	162	26.13
Transaldolase 1 (Taldo1)	3,997	10,441	0.38	6,234	13,308	0.47
NADH dehydrogenase 1 alpha-5 (Ndufa5)	3,923	83	47.43	4,170	73	57.12
Cytochrome *c* oxidase Va (Cox5a)	3,901	452	8.63	2,557	252	10.13
cAMP-regulated phosphoprotein 19 (Arpp19)	3,899	15,608	0.25	2,628	7,132	0.37
Proteasome 26S subunit 3 (Psmd3)	3,880	556	6.97	4,621	85	54.34
Cytochrome *c* oxidase subunit IV-1 (Cox4i1)	3,864	79	49.04	3,441	77	44.59
Amino-terminal enhancer of split (Aes)	3,864	1,287	3.00	3,421	750	4.56
Proteasome beta-3 (Psmb3)	3,860	2,610	1.48	5,159	152	33.89
Myelocytomatosis viral oncogene- (Myc)	3,854	792	4.86	3,028	508	6.00
LIM domain only 4 (Lmo4)	3,812	322	11.85	4,896	413	11.85
Cyclin-dependent kinase 4 (Cdk4)	3,807	639	5.96	4,695	942	4.98
Spastic paraplegia 21 (Spg21)	3,786	3,421	1.11	3,641	1,351	2.69
Proteasome alpha-6 (Psma6)	3,740	311	12.03	4,015	81	49.56
FK506 binding protein 1a (Fkbp1a)	3,734	91	41.26	3,195	91	35.06
Cold shock domain protein A (Csda)	3,682	107	34.45	4,488	81	55.40
Neural precursor cell expressed, developmentally downregulated 8 (Nedd8)	3,674	4,705	0.78	2,801	9,675	0.29
Rho GDP dissociation inhibitor (GDI) alpha	3,662	202	18.11	5,106	95	53.74
Guanine nucleotide binding protein α inhibitor 2 (Gnai2)	3,635	1,846	2.00	3,602	1,399	2.57
Peroxiredoxin 5 (Prdx5)	3,602	71	51.07	3,060	71	43.09
DnaJ (Hsp40)subfamily A-2 (Dnaja2)	3,586	76	47.44	5,134	78	65.61
Spermidine/spermine N^1-acetyl transferase (Sat)	3,571	7,332	0.49	3,937	15,500	0.25

Table W5. (*continued*)

mRNA	Mean Signal Strength*		ASML^{wt} Exosomes *versus* Cells	Mean Signal Strength*		ASML-CD44v^{kd} Exosomes *versus* Cells
	ASML^{wt}			ASML-CD44v^{kd}		
	Exosomes	Cells		Exosomes	Cells	
CD24	3,455	2,353	1.47	4,445	3,541	1.26
Aldo-keto reductase 1-B8 (Akr1b8)	3,432	30,153	0.11	1,313	6,794	0.19
Annexin A4 (Anxa4)	3,421	101	33.83	4,578	90	50.94
Tubulin alpha 1 (Tuba1)	3,388	28,924	0.12	5,870	14,869	0.39
Galactokinase 1 (Galk1)	3,366	91	37.19	4,419	95	46.51
ARP10 actin-related protein 10 (Actr10)	3,336	11,666	0.29	4,332	5,793	0.75
S-adenosylhomocysteine hydrolase (Ahcy)	3,328	nd	∞	2,459	nd	∞
NADH dehydrogenase 1 alpha 11 (Ndufa11)	3,324	180	18.49	3,244	155	20.87
t-complex protein 1 (Tcp1)	3,294	25,709	0.13	3,109	21,769	0.14
Phosphoserine phosphatase (Psph)	3,287	107	30.75	3,115	94	33.01
Inosine 5-monophosphate dehydrog.2 (Impdh2)	3,261	nd	∞	2,763	nd	∞
Chaperonin subunit 3 (Cct3)	3,249	5,753	0.56	4,492	5,955	0.75
Protein phosphatase 2a alpha (Ppp2ca)	3,218	2,402	1.34	3,835	2,353	1.63
Upregulated by 1,25-dihydroxyvitamin D-3 (Txnip)	3,214	3,492	0.92	6,130	6,039	1.02
Microtubule-associated protein light chain 1A/1B light 3 (Map1lc3b)	3,176	1,438	2.21	6,066	449	13.51
Glucose phosphate isomerase (Gpi)	3,158	71	44.78	3,444	87	39.39
Annexin A5 (Anxa5)	3,115	5,634	0.55	2,642	3,566	0.74
Coated vesicle membrane protein (Rnp24)	3115	nd	∞	2,593	nd	∞
Peroxiredoxin 6 (Prdx6)	3,108	74	41.98	3,706	67	55.54
GDP dissociation inhibitor 2 (Gdi2)	3,077	70	44.24	5,625	69	81.43
Cytochrome *c* oxidase subunit Vb (Cox5b)	3,037	83	36.46	2,219	74	30.19
MAP kinase-interacting serine/threonine kinase 2 (Mknk2)	3,025	nd	∞	3,221	nd	∞

*mRNA was ordered according to the signal strength in ASML^{wt} exosomes (mean signal strength was calculated from duplicates, respectively, triplicates, after normalization of two independently performed microarray analyses. Only defined mRNA with a mean signal strength of >3000 was included.
[†]nd: below the detection limit in cell extract. There has been no ASML-CD44v^{kd} mRNA opposing regulated in cells *versus* exosomes.
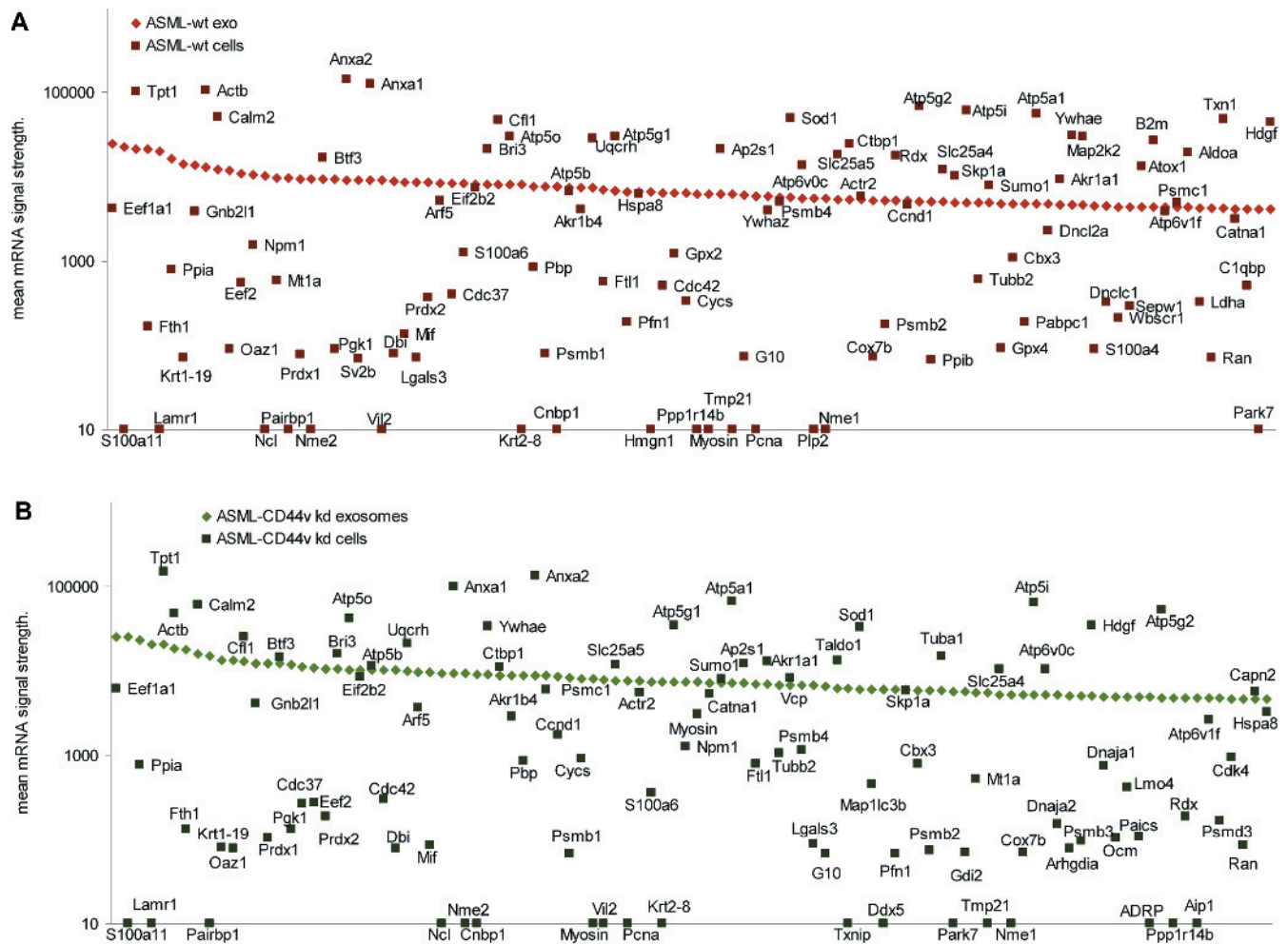
Figure W1. Comparison of ASML[wt] and ASML-CD44v[kd] exosomal *versus* cellular mRNA. (A) The 100 exosomal ASML[wt] mRNAs with the highest signal strength and, for comparison, the corresponding cellular mRNAs and (B) the 100 exosomal ASML-CD44v[kd] mRNAs with the highest signal strength and, for comparison, the corresponding cellular mRNAs are shown. The mean signal strength of duplicates, respectively, triplicates, of two independent microarray analyses is shown. For more detailed information and full names, see Table W5. Independent of CD44v expression, the composition of exosomal and cellular mRNAs differs strongly.
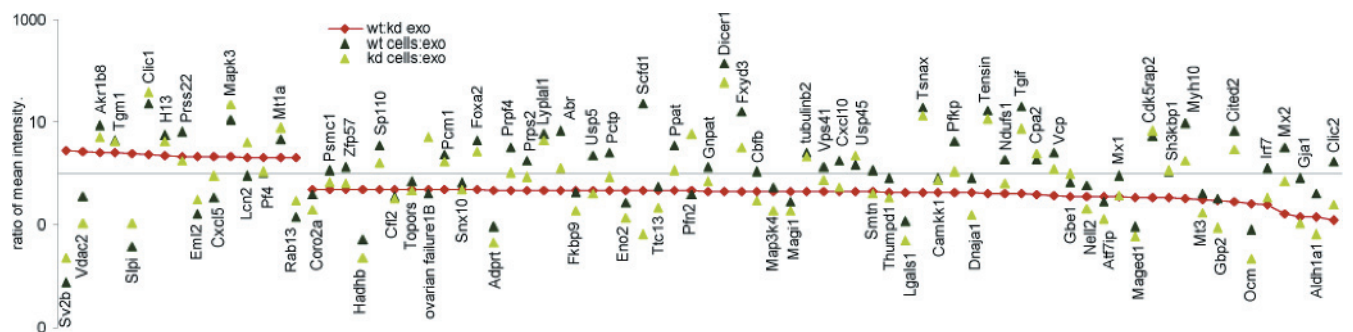

Figure W2. Comparison of the ratio of exosomal ASML[wt] to ASML-CD44v[kd] mRNA with the ratio of cellular to exosomal mRNA: Scatter blot of exosomal mRNA that differs more than two-fold between ASML[wt] *versus* ASML-CD44v[kd] exosomes as well as the ratios of the ASML[wt] and ASML-CD44v[kd] cellular to exosomal mRNA. For abbreviations, see Tables W4 and W5. With four exceptions (ovarian failure1B, Scfd1, Pfn2, and Clic2), signals for both ASML[wt] and ASML-CD44v[kd] cellular mRNA are either enriched or reduced compared to the exosomal mRNA signal strength. This finding strongly argues against CD44v being directly engaged in mRNA recruitment into MVB.
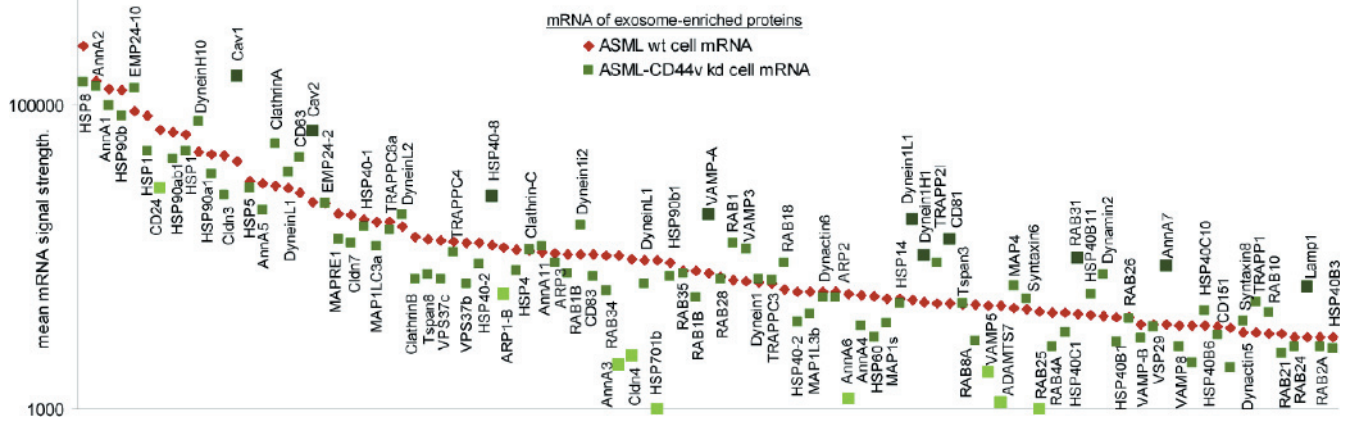
Figure W3. Comparison of cellular ASML^{wt} and ASML-CD44v^{kd} mRNA whose proteins are enriched in exosomes: Scatter blot of mean cellular mRNA signal strength in ASML^{wt} and ASML-CD44v^{kd} cells. Only mRNAs whose proteins are known to be enriched in exosomes are shown, where from 164 mRNAs the 100 with high signal strength have been selected. The mean signal strength of duplicates, respectively, triplicates, of two independent microarray analyses is shown. mRNAs with a more than two-fold change in the signal strength between ASML^{wt} *versus* ASML-CD44^{kd} cells are indicated by larger symbols. For abbreviations, see Table W3. In comparison to the impact of CD44v on the total cellular mRNA, CD44v rather abundantly affects mRNA, where translation products are enriched in exosomes.

Table W6. miRNA in ASML^wt and ASML-CD44v^kd Exosomes and Cells.

(A) Exosomal miRNA

miRNA	Mean Signal Strength*		ASML^wt/ASML-CD44v^kd Exosomes
	ASML^wt	ASML-CD44v^kd	
	Exosomes		
let-7a	2,710	2,808	0.97
let-7b	5,038	14,760	0.34^†
let-7c	24,097	29,257	0.82
let-7d	1,148	377	3.04^†
let-7e	12,646	32,111	0.39^†
let-7f	961	971	0.99
let-7i	346	561	0.62
miR-101b	285	853	0.33^†
miR-103	1,468	637	2.30^†
miR-106b	1,520	2,228	0.68
miR-10a-3p	425	484	0.88
miR-10a-5p	166	445	0.37^†
miR-122	236	400	0.59
miR-124	2,332	1,163	2.00^†
miR-125a-3p	1,574	1,815	0.87
miR-125a-5p	9,079	2,077	4.37^†
miR-125b-3p	29,549	5,541	5.33^†
miR-125b-5p	2,144	1,825	1.18
miR-127	1,209	356	3.40^†
miR-129	15,607	7,956	1.96
miR-130b	3,032	2,086	1.45
miR-138	1,791	3,036	0.59
miR-142-5p	541	990	0.55
miR-147	337	496	0.68
miR-148b-3p	1,924	528	3.64^†
miR-150	2,415	2,151	1.12
miR-183	429	292	1.47
miR-184	5,936	7,438	0.80
miR-185	655	1,510	0.43^†
miR-193	416	191	2.17^†
miR-196a	293	416	0.70
miR-200b	492	339	1.45
miR-200c	697	511	1.36
miR-204	24,335	23,711	1.03
miR-206	6,513	4,944	1.32
miR-207	4,876	8,012	0.61
miR-208	686	941	0.73
miR-21	11,462	5,333	2.15^†
miR-214	9,826	3,482	2.82^†
miR-22	427	945	0.45^†
miR-221	1,421	979	1.45
miR-222	848	909	0.93
miR-23a	692	754	0.92
miR-23b	1,401	1,120	1.25
miR-24	35,571	6,978	5.10^†
miR-26b	7,022	26,350	0.27
miR-290	12,052	11,948	1.01
miR-291a-5p	5,534	627	8.83^†
miR-296	33,359	9,235	3.61^†
miR-298	266	454	0.59
miR-29a	1,808	911	1.99
miR-29b	1,281	676	1.90
miR-29c	1,118	533	2.10^†
miR-300-3p	1,951	1,213	1.61
miR-300-5p	65,490	7,287	8.99^†
miR-30b-3p	2,348	5,402	0.43^†
miR-30b-5p	345	401	0.86
miR-30c	5,715	1,870	3.06^†
miR-31	533	563	0.95
miR-323	1,910	964	1.98
miR-325-3p	7,129	5,608	1.27
miR-325-5p	522	1,617	0.32^†
miR-327	463	392	1.18
miR-329	745	1,048	0.71
miR-330	285	1,181	0.24^†
miR-331	585	4,471	0.13
miR-341	13,956	9,369	1.49
miR-342-5p	404	999	0.40^†
miR-347	801	1,084	0.74
miR-34a	650	5,420	0.12^†

(A) Exosomal miRNA

miRNA	Mean Signal Strength*		ASML^wt/ASML-CD44v^kd Exosomes
	ASML^wt	ASML-CD44v^kd	
	Exosomes		
miR-34c	410	565	0.72
miR-350	245	455	0.54
miR-351	3,707	1,558	2.38^†
miR-352	435	525	0.83
miR-361	777	950	0.82
miR-363	1,692	181	9.34^†
miR-370	98	579	0.17^†
miR-377	324	753	0.43^†
miR-381	433	480	0.90
miR-382	18,070	3,630	4.98^†
miR-409-5p	375	1,801	0.21^†
miR-423	4,548	1,448	3.14^†
miR-466c	403	674	0.60
miR-471	432	826	0.52
miR-494	31,123	14,605	2.13^†
miR-500	1,225	548	2.24^†
miR-503	14,520	7,329	1.98
miR-540	378	578	0.66
miR-542-3p	14,225	2,133	6.67^†
miR-542-5p	463	213	2.18^†
miR-551b	1,794	2,050	0.87
miR-652	436	129	3.38^†
miR-664	386	592	0.65
miR-743a	247	611	0.40^†
miR-743b	277	497	0.56
miR-7a	569	5,188	0.11^†
miR-872	851	706	1.21
miR-874	3,096	1,075	2.88^†
miR-877	4,763	4,625	1.03
miR-96	417	118	3.54^†
miR-98	453	559	0.81
miR-99b	1,359	5,133	0.26^†

(B) Cellular miRNA

miRNA	Mean Signal Strength*		ASML^wt/ASML-CD44v^kd Cells
	ASML^wt	ASML-CD44v^kd	
	Cells		
let-7a	13,560	15,699	0.86
let-7b	7,125	10,683	0.67
let-7c	7,963	15,121	0.53
let-7d	6,440	5,844	1.10
let-7e	1,158	3,018	0.38^†
let-7f	15,565	16,357	0.95
let-7i	4,485	5,129	0.87
miR-100	935	1,401	0.67
miR-101b	700	488	1.43
miR-103	2,369	2,380	1.00
miR-106b	4,409	4,475	0.99
miR-107	2,664	2,503	1.06
miR-10a-5p	5,116	6,966	0.73
miR-1224	992	566	1.75
miR-125a-5p	630	1,424	0.44^†
miR-125b-5p	32,799	46,281	0.71
miR-128	491	429	1.15
miR-130a	3,199	5,535	0.58
miR-130b	1,396	1,288	1.08
miR-140	689	814	0.85
miR-141	1,744	607	2.87^†
miR-148b-3p	501	466	1.08
miR-151	857	1,056	0.81
miR-15b	5,295	5,005	1.06
miR-16	10,127	9,008	1.12
miR-181c	428	708	0.60
miR-181d	453	467	0.97
miR-182	948	845	1.12
miR-183	1,854	2,431	0.76

Table W6. (*continued*)

(B) Cellular miRNA

miRNA	Mean Signal Strength*		ASML^wt/ASML-CD44v^kd Cells
	ASML^wt	ASML-CD44v^kd	
	Cells		
miR-185	749	432	1.73
miR-186	1,606	610	2.63[†]
miR-193	329	498	0.66
miR-1949	2,018	614	3.29[†]
miR-196c	793	456	1.74
miR-200a	2,646	560	4.73[†]
miR-200b	4,467	949	4.71[†]
miR-200c	1,192	186	6.40[†]
miR-203	1,524	2,645	0.58
miR-207	286	523	0.55
miR-21	57,732	47,159	1.22
miR-210	747	1,056	0.71
miR-218a	307	548	0.56
miR-22	4,177	5,884	0.71
miR-221	2,233	5,340	0.42
miR-222	1,217	1,459	0.83
miR-23a	12,378	22,556	0.55
miR-23b	4,652	5,909	0.79
miR-24	6,898	13,293	0.52
miR-25	4,572	3,947	1.16
miR-26a	3,053	4,094	0.75
miR-26b	2,252	3,084	0.73
miR-27a	4,819	12,832	0.38[†]
miR-27b	2,823	3,969	0.71
miR-28	555	431	1.29
miR-29a	37,744	37,658	1.00
miR-29b	11,953	24,913	0.48[†]
miR-29c	2,719	2,862	0.95
miR-301a	469	1,559	0.30[†]
miR-30a	928	1,013	0.92
miR-30b-5p	1,262	1,222	1.03
miR-30c	2,404	2,207	1.09
miR-30d	492	478	1.03
miR-30e	1,160	1,407	0.82
miR-31	8,921	1,2526	0.71
miR-32	378	623	0.61

Table W6. (*continued*)

(B) Cellular miRNA

miRNA	Mean Signal Strength*		ASML^wt/ASML-CD44v^kd Cells
	ASML^wt	ASML-CD44v^kd	
	Cells		
miR-322	614	453	1.36
miR-324-3p	971	1,041	0.93
miR-335	433	531	0.82
miR-34a	597	1,305	0.46[†]
miR-34b	669	355	1.89
miR-34c	720	320	2.25[†]
miR-361	414	436	0.95
miR-365	1,493	1,426	1.05
miR-374	539	418	1.29
miR-425	386	547	0.71
miR-429	2,625	544	4.83[†]
miR-466b-1	1,129	1,481	0.76
miR-466b-2	1,296	1,643	0.79
miR-466c	1,015	1,430	0.71
miR-485	312	579	0.54
miR-494	707	417	1.70
miR-500	432	457	0.95
miR-582	407	92	4.44[†]
miR-652	1,366	1,756	0.78
miR-672	394	1,063	0.37[†]
miR-741-3p	11	857	0.01[†]
miR-764	312	647	0.48[†]
miR-7a	1,850	373	4.96[†]
miR-872	692	748	0.92
miR-883	7	438	0.02[†]
miR-9	486	387	1.25
miR-93	1,936	1,727	1.12
miR-96	5,737	5,758	1.00
miR-98	1,139	1,932	0.59
miR-99a	152	4,253	0.04[†]
miR-99b	528	891	0.59

*All miRNAs (in alphabetic order) with a mean signal strength (quadruplicates, two independently performed microarray analyses) after normalization (Chipster analysis and Agilent annotation by Agilent Feature Extraction software) of >400 in ASML^wt or ASML-CD44v^kd exosomes or cells are shown.
[†]miRNA that differs between ASML^wt *versus* ASML-CD44v^kd exosomes or cells in signal intensity by more than two-fold.
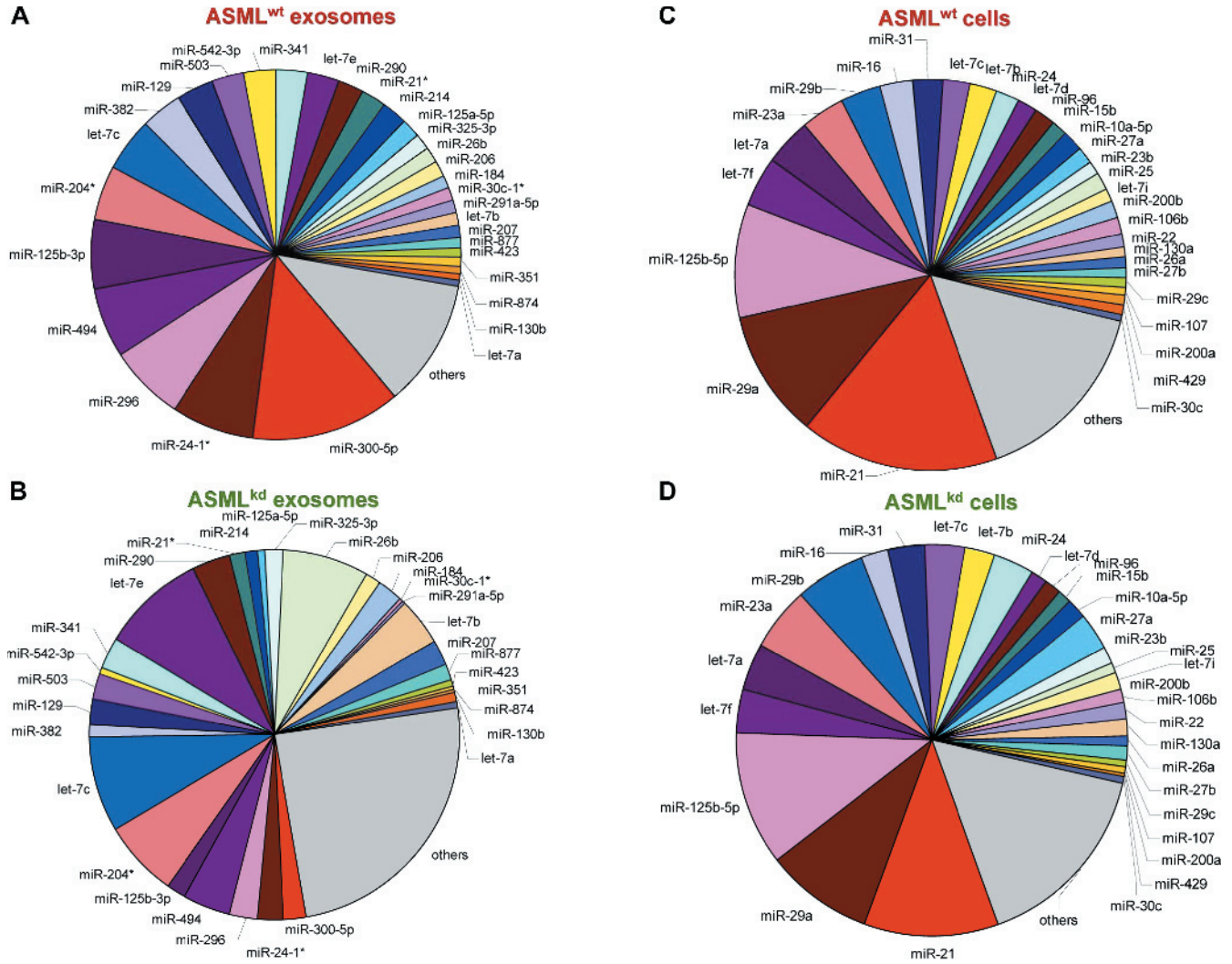
Figure W4. Comparative analysis of ASML^wt and ASML-CD44v^kd cellular and exosomal miRNAs. (A–D) Presentation of the most abundant miRNA in ASML^wt and, for comparison, in ASML-CD44v^kd cells and exosomes. The mean signal strength of quadruplicates of two independent microarray analyses is shown. ASML exosomes and cells contain a limited number of miRNA that differ significantly between cells and exosomes and in dependence on CD44v expression.
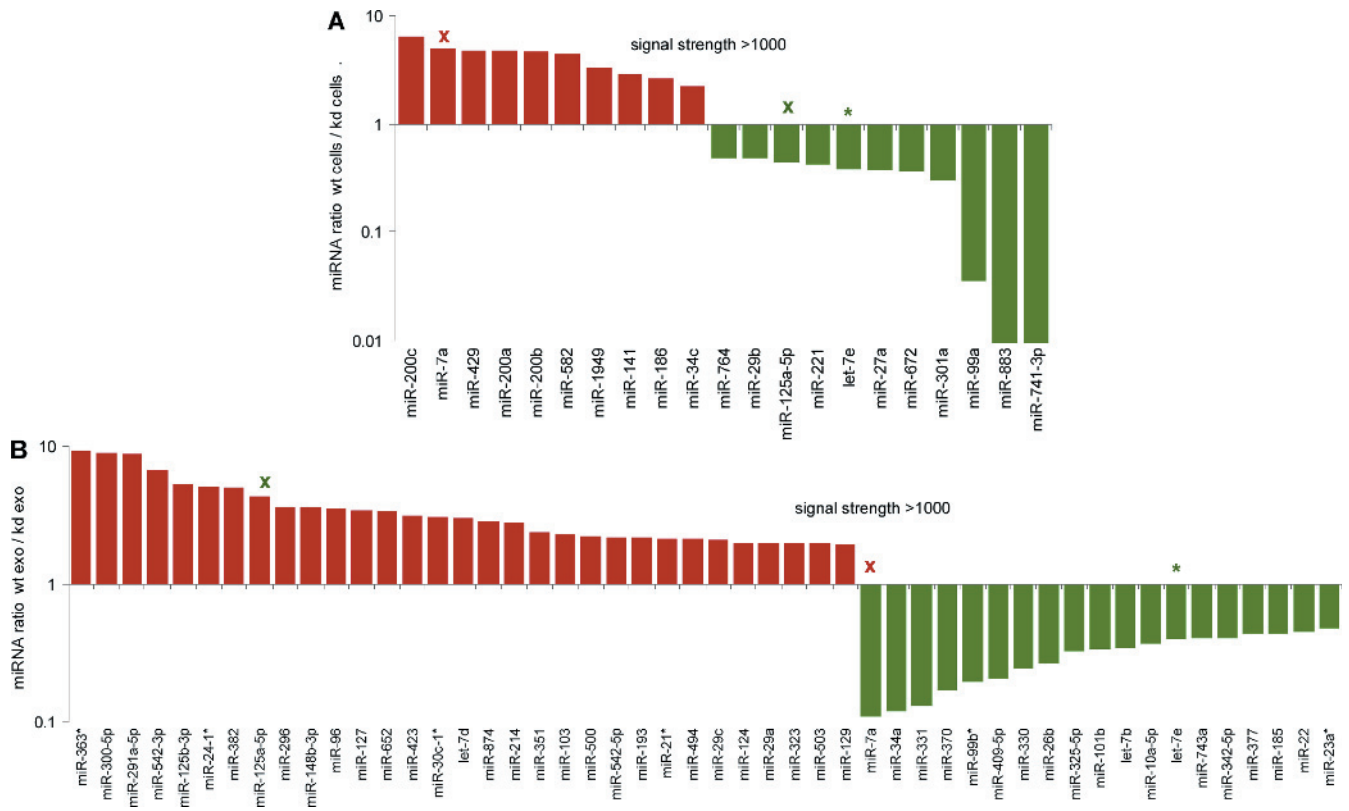
Figure W5. Comparison of miRNA in ASML[wt] *versus* ASML-CD44v[kd] cells and exosomes. (A) Cellular and (B) exosomal miRNAs with a signal strength > 1000 and a more than two-fold difference in signal strength in ASML[wt] *versus* ASML-CD44v[kd] cells or exosomes (mean signal strength of quadruplicates of two independent microarray analyses) is shown; Opposingly regulated miRNA in cells *versus* exosomes are indicated by X and alike regulated miRNA by asterisk. Independent of CD44v expression, most abundantly recovered cellular and exosomal miRNAs differ significantly, confirming the selectivity of miRNA recruitment.
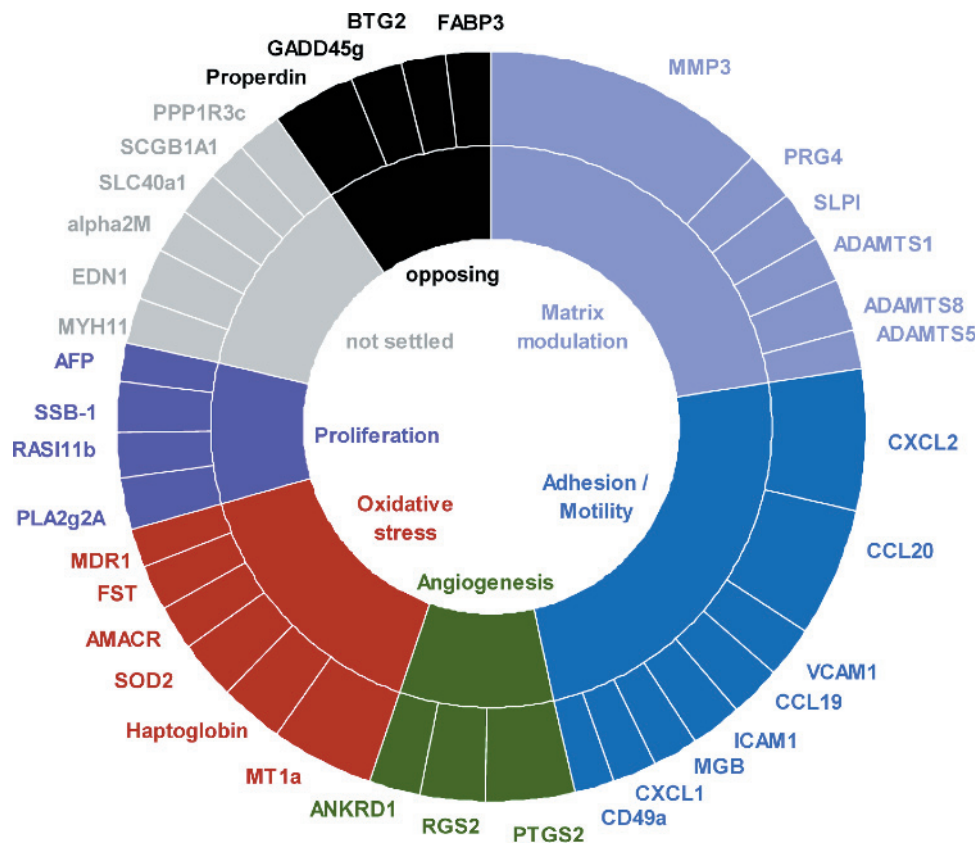
Figure W6. Exosome transfer–promoted activities of target cells in the premetastatic niche. Exosome uptake–induced upregulated mRNAs in LnStr were grouped according to main functional activities and are presented according to the fold up-regulation. Short comments on the main activity of upregulated genes and related references are given below.

Matrix modulation

MMP3 (matrix metallopeptidase 3): matrix degradation, well organized role in invasion and metastasis

Hua H, Li M, Luo T, Yin Y, and Jiang Y (2011). Matrix metalloproteinases in tumorigenesis: an evolving paradigm. *Cell Mol Life Sci* **68**, 3853–3868.

PRG4 (proteoglycan 4): co-receptor for integrins, co-operates with MT1-MMP in collagen modulation.

Vuoriluoto K, Högnäs G, Meller P, Lehti K, and Ivaska J (2011). Syndecan-1 and -4 differentially regulate oncogenic K-ras dependent cell invasion into collagen through α2β1 integrin and MT1-MMP. *Matrix Biol* **30**, 207–217.

SLPI (secretory leukocyte peptidase inhibitor): often upregulated in cancer, induces MMP9 transcription.

Nukiwa T, Suzuki T, Fukuhara T, and Kikuchi T (2008). Secretory leukocyte peptidase inhibitor and lung cancer. *Cancer Sci* **99**, 849–855.
Hoskins E, Rodriguez-Canales J, Hewitt SM, Elmasri W, Han J, Han S, Davidson B, and Kohn EC (2011). Paracrine SLPI secretion upregulates MMP-9 transcription and secretion in ovarian cancer cells. *Gynecol Oncol* **122**, 656–662.

ADAMTS1 (a disintegrin-like and metalloprotease with thrombospondin type 1, motif 1); ADAMTS8 (a disintegrin-like and metalloprotease with thrombospondin type 1, motif 8); ADAMTS5 (a disintegrin-like and metalloprotease with thrombospondin type 1, motif 5): procollagen maturation, extracellular matrix proteolysis related to angiogenesis and metastasis.

Apte SS (2009). A disintegrin-like and metalloprotease (reprolysin-type) with thrombospondin type 1 motif (ADAMTS) superfamily: functions and mechanisms. *J Biol Chem* **284**, 31493–31497.

Adhesion/motility

CXCL2 (C-X-C chemokine ligand 2), CCL20 (C-C chemokine ligand 20), CCL19 (C-C chemokine ligand 19), CXCL1 (CXC chemokine ligand 1): chemokines and their ligands largely determine organ specificity of metastases, facilitating migration and extravasation; they can be involved in tumor cell proliferation and survival.

Ben-Baruch A (2008). Organ selectivity in metastasis: regulation by chemokines and their receptors. *Clin Exp Metastasis* **25**, 345–356.

VCAM1 (vascular cell adhesion molecule 1); ICAM1 (intercellular adhesion molecule 1): metastasis promoting by engagement in migration, proliferation, angiogenesis, and thrombosis.

Mousa SA (2008). Cell adhesion molecules: potential therapeutic & diagnostic implications. *Mol Biotechnol* **38**, 33–40.

MGP (matrix Gla protein): migration promoting, overexpressed in cancer.

Mertsch S, Schurgers LJ, Weber K, Paulus W, and Senner V (2009). Matrix gla protein (MGP): an overexpressed and migration-promoting mesenchymal component in glioblastoma. *BMC Cancer* **9**, 302.

CD49a (integrin alpha 1): supports tumor cell migration.

Madsen CD and Sahai E (2010). Cancer dissemination—lessons from leukocytes. *Dev Cell* **19**, 13–26.

Angiogenesis

PTGS2/COX2 (prostaglandin-endoperoxide synthase 2): involved in inflammation, increased in more aggressive forms of colorectal cancer, known to promote angiogenesis.

Wang S, Liu Z, Wang L, and Zhang X (2009). NF-kappaB signaling pathway, inflammation and colorectal cancer. *Cell Mol Immunol* **6**, 327–334.

RGS2 (regulator of G-protein signaling 2): critical regulator of proangiogenic function of MDSC.

Boelte KC, Gordy LE, Joyce S, Thompson MA, Yang L, and Lin PC (2011). Rgs2 mediates pro-angiogenic function of myeloid derived suppressor cells in the tumor microenvironment via upregulation of MCP-1. *PLoS One* **6**, e18534.

ANKRD1 (ankyrin repeat domain 1): co-transcription factor involved in angiogenesis.

Samaras SE, Shi Y, and Davidson JM (2006). CARP: fishing for novel mechanisms of neovascularization. *J Investig Dermatol Symp Proc* **11**, 124–131.

Oxidative stress

MT1a (metallothionein): contributes to protective reactions with chemotherapeutic agents that are electrophiles or can generate reactive oxygen species.

Namdarghanbari M, Wobig W, Krezoski S, Tabatabai NM, and Petering DH (2011). Mammalian metallothionein in toxicology, cancer, and cancer chemotherapy. *J Biol Inorg Chem* **16**, 1087–1101.

Haptoglobin: CD163 clearance and metabolism of "free" hemoglobin released during intravascular hemolysis. This scavenging system counteracts the potentially harmful oxidative and NO-scavenging effects associated with "free" hemoglobin.

Nielsen MJ and Moestrup SK (2009). Receptor targeting of hemoglobin mediated by the haptoglobins: roles beyond heme scavenging. *Blood* **114**, 764–771.

SOD2 (superoxide dismutase 2): catalysis oxidative stress, upregulated in metastasis.

Hempel N, Carrico PM, and Melendez JA (2011). Manganese superoxide dismutase (Sod2) and redox-control of signaling events that drive metastasis. *Anticancer Agents Med Chem* **11**, 191–201.

AMACR (α-methylacyl-CoA racemase): catalyzes the chiral inversion of a diverse number of 2-methyl acids (as their CoA esters) and regulates the entry of branched-chain lipids into the peroxisomal and mitochondrial β-oxidation pathways; linked with prostate, breast, colon, and other cancers.

Lloyd MD, Darley DJ, Wierzbicki AS, and Threadgill MD (2008). Alpha-methylacyl-CoA racemase—an 'obscure' metabolic enzyme takes centre stage. *FEBS J* **275**, 1089–1102.

FST (follistatin): Localization of FST to the nucleolus attenuates rRNA synthesis, a key process for cellular energy homeostasis and cell survival. Overexpression of FST delays glucose deprivation–induced apoptosis and promotes survival.

Gao X, Wei S, Lai K, Sheng J, Su J, Zhu J, Dong H, Hu H, and Xu Z (2010). Nucleolar follistatin promotes cancer cell survival under glucose-deprived conditions through inhibiting cellular rRNA synthesis. *J Biol Chem* **285**, 36857–36864.

MDR1 (ATP-binding cassette, subfamily B, member 1): promotes drug resistance, high expression frequently associated with metastasizing cancer-initiating cells.

Adhikari AS, Agarwal N, and Iwakuma T (2011). Metastatic potential of tumor-initiating cells in solid tumors. *Front Biosci* **16**, 1927–1938.

Proliferation

PLA2g2A (phospholipase A2, group 2A): contributes to EGFR activation.

Hernández M, Martín R, García-Cubillas MD, Maeso-Hernández P, and Nieto ML (2010). Secreted PLA2 induces proliferation in astrocytoma through the EGF receptor: another inflammation-cancer link. *Neuro Oncol* **12**, 1014–1023.

RASL11b (RAS-like family 11 member B): RasL11b acts in concert with UBF to facilitate initiation and/or elongation by RNA polymerase II, suggested to be upregulated in cancer.

Stolle K, Schnoor M, Fuellen G, Spitzer M, Cullen P, and Lorkowski S (2010). Cloning, genomic organization, and tissue-specific expression of the RASL11B gene. *Biochim Biophys Acta* **1769**, 514–524.

Pistoni M, Verrecchia A, Doni M, Guccione E, and Amati B (2010). Chromatin association and regulation of rDNA transcription by the Ras-family protein RasL11a. *EMBO J* **29**, 1215–1224.

SSB1 (similar to SPRY domain-containing SOCS box protein): binds to MET and enhances the HGF-induced Erk–Elk-1–SRE pathway.

Wang D, Li Z, Messing EM, and Wu G (2005). The SPRY domain-containing SOCS box protein 1 (SSB-1) interacts with MET and enhances the hepatocyte growth factor-induced Erk-Elk-1-serum response element pathway. *J Biol Chem* **280**, 16393–16401.

AFP (alpha-fetoprotein): tumor growth enhancing, possesses proangiogenic properties.

Mizejewski GJ (2007). Physiology of alpha-fetoprotein as a biomarker for perinatal distress: relevance to adverse pregnancy outcome. *Exp Biol Med* **232**, 993–1004.

Not settled

MYH11 (myosin heavy chain 11): not settled, known to fuse with CBF in leukemia.

Weckerle AB, Santra M, Ng MC, Koty PP, and Wang YH (2011). *CBFB* and *MYH11* in inv(16)(p13q22) of acute myeloid leukemia displaying close spatial proximity in interphase nuclei of human hematopoietic stem cells. *Genes Chromosomes Cancer* **50**, 746–755.

EDN1 (endothelin 1): not settled, peptide hormone signaling through its cognate receptor, the endothelin-A receptor, critical for patterning, relation to cancer unknown.

Clouthier DE, Garcia E, and Schilling TF (2010). Regulation of facial morphogenesis by endothelin signaling: insights from mice and fish. *Am J Med Genet A* **152A**, 2962–2973.

α2M (alpha-2-macroglobulin): interacts and captures virtually any proteinase.

Woessner JF Jr (1991). Matrix metalloproteinases and their inhibitors in connective tissue remodeling. *FASEB J* **5**, 2145–2154.

SLC40a1 (solute carrier family 39 iron-regulated transporter, member 1): iron export, may inhibit metastasis.

Jiang XP, Elliott RL, and Head JF (2010). Manipulation of iron transporter genes results in the suppression of human and mouse mammary adenocarcinomas. *Anticancer Res* **30**, 759–765.

SCGB1A1 (secretoglobin, family 1A, member 1): downstream target for a homeodomain transcription factor NKX2-1, which is critical for the development of lung, thyroid, and ventral forebrain, upregulated in lung cancer.

Kurotani R, Kumaki N, Naizhen X, Ward JM, Linnoila RI, and Kimura S (2011). Secretoglobin 3A2/uteroglobin-related protein 1 is a novel marker for pulmonary carcinoma in mice and humans. *Lung Cancer* **71**, 42–48.

PPP1R3C (protein phosphatase 1, regulatory (inhibitor) subunit 3C): correlates with glycogen accumulation under hypoxia, described as a candidate tumor suppressor.

Shen GM, Zhang FL, Liu XL, and Zhang JW (2010). Hypoxia-inducible factor 1-mediated regulation of PPP1R3C promotes glycogen accumulation in human MCF-7 cells under hypoxia. *FEBS Lett* **584**, 4366–4372.

Bonazzi VF, Irwin D, and Hayward NK (2009). Identification of candidate tumor suppressor genes inactivated by promoter methylation in melanoma. *Genes Chromosomes Cancer* **48**, 10–21.

Metastasis opposing

Properdin: antiangiogenic.

Kemper C, Atkinson JP, and Hourcade DE (2010). Properdin: emerging roles of a pattern-recognition molecule. *Annu Rev Immunol* **28**, 131–155.

GADD45g (growth arrest and DNA-damage-inducible 45γ): supposed to function as metastasis inhibitor.

Ying J, Srivastava G, Hsieh WS, Gao Z, Murray P, Liao SK, Ambinder R, and Tao Q (2005). The stress-responsive gene GADD45G is a functional tumor suppressor, with its response to environmental stresses frequently disrupted epigenetically in multiple tumors. *Clin Cancer Res* **11**, 6442–6449.

BTG2 (B-cell translocation gene 2): antiproliferative, pan cell cycle modulator and endogenous cell death molecule, downregulated in cancer.

Lim IK (2006). TIS21 (/BTG2/PC3) as a link between ageing and cancer: cell cycle regulator and endogenous cell death molecule. *J Cancer Res Clin Oncol* **132**, 417–426.

FABP3 (fatty acid binding protein 3): inhibits proliferation and promotes apoptosis

Zhu C, Hu DL, Liu YQ, Zhang QJ, Chen FK, Kong XQ, Cao KJ, Zhang JS, and Qian LM (2011). Fabp3 inhibits proliferation and promotes apoptosis of embryonic myocardial cells. *Cell Biochem Biophys* **60**, 259–266.
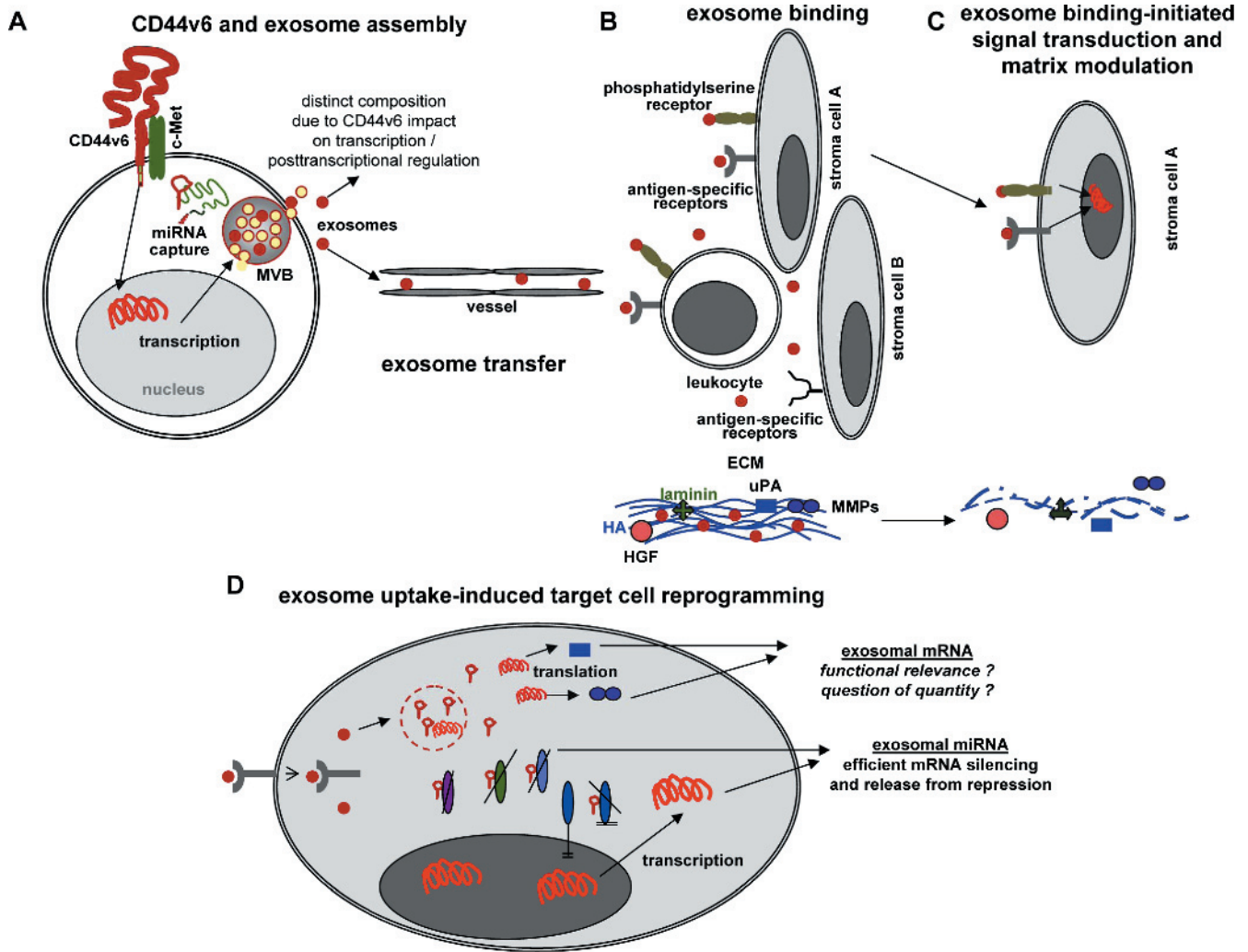
Figure W7. A metastasis-associated gene, its impact on exosome shaping, and the impact on host cells: (A) CD44v6 influences gene transcription and posttranscription modulation. This influences the protein [1,2], mRNA, and miRNA composition of exosomes. Exosomes reach premetastatic organs from a distantly located primary tumor (demonstrated for draining lymph nodes, accounts equally for other metastatic organs and the bone marrow, as well as for transfer through the blood [2,3]). (B) Exosomes bind selected target cells (demonstrated for LnStr and LuFb, additional preferred targets for ASML exosomes are monocytes/monocyte progenitors [3]). (C) Exosome binding is supposed to initiate signal transduction in target cells [4] (not approached in the present manuscript) and severely affect the host matrix (unpublished). (D) Exosomes are taken up and uptaken mRNA and miRNA are recovered in the target cell. According to our findings, uptaken miRNA severely modulates the target cell, fitting the demands for premetastatic niche formation (only demonstrated for metastatic organ stroma cells but accounts equally well for hematopoietic cells).

Taken that tumor exosomes are recovered in patients' sera [5] and exhibit very selective binding implies that functional activity of exosomes has to be taken into account at sites distant from the tumor (e.g., premetastatic organs), where the selectivity of exosome uptake will greatly facilitate therapeutic interference. However and notably, as the exosome composition becomes significantly influenced also by proteins of the tumor cell that are not engaged in exosome assembly or transport, it is essential to characterize the individual patient's exosomes in advance, which can be approached by tumor exosomes in the patient's serum.

[1] Jung T, Castellana D, Klingbeil P, Cuesta Hernández I, Vitacolonna M, Orlicky DJ, Roffler SR, Brodt P, and Zöller M (2009). CD44v6 dependence of premetastatic niche preparation by exosomes. *Neoplasia* **11**, 1093–1105.

[2] Zech D, Rana S, Büchler MW, and Zöller M (2012). Tumor-exosomes and leukocyte activation: an ambivalent crosstalk. *Cell Commun Signal* **10**, 37.

[3] Rana S, Shijing Y, Stadel D, and Zöller M (2012). Toward tailored exosomes: The exosomal tetraspanin web contributes to target cell selection. *Int J Biochem Cell Biol* **44**, 1574–1584.

[4] Hupalowska A and Miaczynska M (2012). The new faces of endocytosis in signaling. *Traffic* **13**, 9–18.

[5] Wittmann J and Jäck HM (2010). Serum microRNAs as powerful cancer biomarkers. *Biochim Biophys Acta* **1806**, 200–207.